Explosive volcanic activity on Venus: The roles of volatile contribution, degassing, and external environment

Airey, M. W. ORCID: https://orcid.org/0000-0002-9784-0043, Mather, T. A., Pyle, D. M., Glaze, L. S., Ghail, R. C. and Wilson, C. F. (2015) Explosive volcanic activity on Venus: The roles of volatile contribution, degassing, and external environment. Planetary and Space Science, 113 - 114. 33 - 48. ISSN 0032-0633 doi: https://doi.org/10.1016/j.pss.2015.01.009 Available at https://centaur.reading.ac.uk/82482/

Planetary and Space Science 113-114 (2015) 33–48

Contents lists available at ScienceDirect

Planetary and Space Science

journal homepage: www.elsevier.com/locate/pss

Explosive volcanic activity on Venus: The roles of volatile contribution, degassing, and external environment

M.W. Airey [a,*], T.A. Mather [a], D.M. Pyle [a], L.S. Glaze [b], R.C. Ghail [c], C.F. Wilson [d]

[a] Dept. of Earth Sciences, University of Oxford, S. Parks Road, Oxford, UK
[b] NASA Goddard Space Flight Center, Greenbelt, MD 20771, USA
[c] Dept. of Civil and Environmental Engineering, Skempton Building, Imperial College London, South Kensington Campus, London, UK
[d] Atmospheric, Oceanic and Planetary Physics, Clarendon Laboratory, University of Oxford, Oxford, UK

ARTICLE INFO

Article history:
Received 28 March 2014
Received in revised form
16 October 2014
Accepted 20 January 2015
Available online 3 February 2015

Keywords:
Venus
Planetary volcanism
Volcano modelling
Conduit processes

ABSTRACT

We investigate the conditions that will promote explosive volcanic activity on Venus. Conduit processes were simulated using a steady-state, isothermal, homogeneous flow model in tandem with a degassing model. The response of exit pressure, exit velocity, and degree of volatile exsolution was explored over a range of volatile concentrations (H_2O and CO_2), magma temperatures, vent altitudes, and conduit geometries relevant to the Venusian environment. We find that the addition of CO_2 to an H_2O-driven eruption increases the final pressure, velocity, and volume fraction gas. Increasing vent elevation leads to a greater degree of magma fragmentation, due to the decrease in the final pressure at the vent, resulting in a greater likelihood of explosive activity. Increasing the magmatic temperature generates higher final pressures, greater velocities, and lower final volume fraction gas values with a correspondingly lower chance of explosive volcanism. Cross-sectionally smaller, and/or deeper, conduits were more conducive to explosive activity. Model runs show that for an explosive eruption to occur at Scathach Fluctus, at Venus' mean planetary radius (MPR), 4.5% H_2O or 3% H_2O with 3% CO_2 (from a 25 m radius conduit) would be required to initiate fragmentation; at Ma'at Mons (~9 km above MPR) only ~2% H_2O is required. A buoyant plume model was used to investigate plume behaviour. It was found that it was not possible to achieve a buoyant column from a 25 m radius conduit at Scathach Fluctus, but a buoyant column reaching up to ~20 km above the vent could be generated at Ma'at Mons with an H_2O concentration of 4.7% (at 1300 K) or a mixed volatile concentration of 3% H_2O with 3% CO_2 (at 1200 K). We also estimate the flux of volcanic gases to the lower atmosphere of Venus, should explosive volcanism occur. Model results suggest explosive activity at Scathach Fluctus would result in an H_2O flux of $\sim 10^7$ kg s^{-1}. Were Scathach Fluctus emplaced in a single event, our model suggests that it may have been emplaced in a period of ~15 days, supplying $1–2 \times 10^4$ Mt H_2O to the atmosphere locally. An eruption of this scale might increase local atmospheric H_2O abundance by several ppm over an area large enough to be detectable by near-infrared nightside sounding using the 1.18 μm spectral window such as that carried out by the Venus Express/VIRTIS spectrometer. Further interrogation of the VIRTIS dataset is recommended to search for ongoing volcanism on Venus.

1. Introduction

Volcanoes and their deposits are some of the most widespread and recognisable geological features in Venus' surface record (Crumpler and Aubele, 2000; Ford et al., 1993; Head et al., 1992; Ivanov and Head, 2011). Volcanic landforms include clusters of small shield volcanoes ranging from < 1 km to 10s of km in diameter ('shield fields'), large volcanoes up to ~1000 km in diameter, steep-sided domes, isolated calderas not associated with an obvious edifice, and stress-induced surface deformation features known as coronae and novae (Head et al., 1992) thought to be associated with shallow magma bodies (McGovern and Solomon, 1998). The broad variety of volcanic features on Venus suggests a corresponding variety of processes responsible for their formation.

Whether or not explosive eruptions occur on Venus has been the subject of debate (e.g. Fagents and Wilson, 1995; Glaze et al., 2011; Thornhill, 1993), as the conditions affecting the physical processes of eruption on Venus are very different to those on Earth. Lava flows have been recognised globally, while pyroclastic density currents and fallout deposits are apparently rare or absent. It has proved difficult to determine the nature of these less common volcanic deposits seen in the radar imagery of Venus and confirmation of an

* Corresponding author. +44 1865 272070.
E-mail address: martin.airey@earth.ox.ac.uk (M.W. Airey).

http://dx.doi.org/10.1016/j.pss.2015.01.009

explosive origin has so far mostly proved to be controversial (Campbell and Rogers, 1994; Grosfils et al., 2011; Keddie and Head, 1995; McGill, 2000). One recent exception is a proposed pyroclastic deposit known as Scathach Fluctus, identified by Ghail and Wilson (2013). This pyroclastic interpretation was arrived at via a combination of radar characteristics, flow morphology, and flow interaction with other geomorphological features.

Establishing whether explosive volcanism occurs on Venus might yield further clues concerning subsurface conditions on Venus and would better inform our understanding of atmospheric processes such as the apparent SO_2 variations detected by Pioneer Venus (Esposito, 1985), and later Venus Express (Marcq et al., 2012). In terms of atmospheric interactions, understanding the heights that explosive plumes might achieve is also key. Our study aims to better understand the eruptive behaviour of volcanoes on Venus through consideration of the factors affecting these processes.

1.1. Explosive volcanism

The processes resulting in terrestrial explosive volcanism have been widely documented in numerous articles on magma ascent dynamics (e.g. Papale et al., 1998; Papale and Polacci, 1999; Wilson et al., 1980; Woods, 1995) and the magma degassing behaviour that leads to it has been extensively modelled (Lesne et al., 2011; Newman and Lowenstern, 2002; Witham et al., 2012). Whether or not explosive volcanism results in a buoyant plume has also been extensively described in previous work on eruption column physics (Sparks, 1986; Valentine and Wohletz, 1989; Wilson et al., 1978; Woods, 1988, 1995; and others). A parcel of magma that decompresses sufficiently and exsolves enough of the volatile gas phase to initiate fragmentation within the conduit, either when the gas volume fraction in the mixture exceeds a critical value (Sparks, 1978), or the magma suffers brittle failure and fragments (Gonnermann and Manga, 2003; Tuffen and Dingwell, 2005), is then emitted from the vent into the overlying atmosphere as a volcanic plume, initially in a momentum-driven 'gas thrust' regime. The column will collapse into a fountain unless enough atmospheric gas can be entrained, heated by the clasts within the plume, expand, and become buoyant. The column is then considered to be in a buoyancy-driven 'convective' regime, and will continue to rise and expand until it reaches the level of neutral buoyancy. At this level, the column spreads laterally in an 'umbrella' region.

The first application of subaerial plume modelling under Venus conditions was carried out by Thornhill (1993); the minimum initial parameter values required for explosive activity were identified by applying the model of Woods (1988) to Venusian environmental conditions. A case study by Robinson et al. (1995) applied the same model to Ma'at Mons and suggested that explosive volcanism could have been responsible for the elevated atmospheric SO_2 concentrations detected by Pioneer Venus (Esposito, 1985). A further suite of studies estimated the overall plume height attainable by explosive volcanic eruption columns over a range of boundary conditions similar to those chosen for this study (Glaze, 1999), and with circular vs. linear vent geometries (Glaze et al., 2011). In this study we link a conduit flow dynamics model, not previously carried out under Venusian conditions, via a jet decompression model, with an established plume dynamics model, which has previously been applied to Venus (Glaze et al., 1997). In addition to this, our model includes CO_2 as an accessory volatile species to H_2O. Previous models only included H_2O but on Venus CO_2 may be of comparatively greater significance in terms of plume dynamics than on Earth when considering the potentially smaller concentration of magmatic H_2O (see Section 1.3) making its inclusion an important innovation.

When conducting an investigation into what may characterise the eruptive style of volcanoes, a broad array of environmental, chemical, and physical factors must be considered. The physical and chemical properties of the atmosphere into which erupted material is injected have a strong control on plume behaviour and cause the process of plume generation to be different on Venus than Earth as do the material properties and the volatile load of the magma.

Table 1
Physical and chemical data for the atmospheres of Venus, Earth, and Mars for comparison. The atmospheric compositions are given in mole fractions with ~0 meaning undetermined but very small. Data from Taylor (2010).

	Venus	*Earth*	*Mars*
Atmosphere			
Molecular weight (g)	43.44	28.98 (dry)	43.49
Surface temperature (K)	730	288	220
Surface pressure (MPa)	9.2	0.1	0.0007
Mass (kg)	4.77×10^{20}	5.30×10^{18}	$\sim 10^{16}$
Composition			
Carbon dioxide	0.96	0.0003	0.95
Nitrogen	0.035	0.770	0.027
Argon	0.00007	0.0093	0.016
Water vapour	~0.0001	~0.01	~0.0003
Oxygen	~0	0.21	0.0013
Sulphur dioxide	150 ppm	0.2 ppb	~0
Carbon monoxide	40 ppm	0.12 ppm	700 ppm
Neon	5 ppm	18 ppm	2.5 ppm

1.2. Environmental conditions on Venus

Venus has a dense CO_2-dominated atmosphere enshrouded in thick sulphuric acid clouds. The atmospheric composition of Venus is provided in Table 1 alongside those of Earth and Mars for comparison. At the mean planetary radius (MPR, ~6051.8 km) the atmospheric pressure is ~9.2 MPa and its temperature is ~730 K due to the high atmospheric density and intense greenhouse effect (Seiff et al., 1985). These factors inhibit explosivity by inhibiting magma fragmentation due to vesiculation, and reducing the plume-atmosphere boundary temperature contrast, respectively. Both the pressure and temperature are strongly altitude dependent, however, and diminish rapidly with altitude into conditions more conducive to plume buoyancy (see Fig. 1). The altitude of the surface of Venus ranges between ~-2 and ~+9 km of the MPR.

The chemical composition of the atmosphere is an important factor since the presence of water vapour can influence column dynamics by releasing latent heat and therefore enhancing buoyancy (Glaze et al., 1997) above the altitude at which it condenses within the plume. This effect, however, is not significant in volcanic plumes on Venus because the atmosphere contains negligible water vapour (see Table 1). The value of the constant g (acceleration due to gravity) is slightly smaller on Venus, 8.41 m s^{-2} as opposed to 9.81 m s^{-2} on Earth, resulting in a smaller effect on pressure and column momentum flux on Venus than on Earth.

1.3. The characteristics of Venus magmas

The chemical composition of magma is important when modelling conduit processes because it affects the viscosity and fluid dynamic response of the decompressing magma flow (Sparks, 1978). With the exception of one anomalous site (Venera 13, which detected alkalic rocks), the bulk geochemical analyses carried out by the Russian Venera and Vega landers (Table 2), at sites located on lava plains and flows characteristic of most (> 70%, Ivanov and Head, 2011) of the planetary surface, are consistent with a weathered basaltic surface composition (Treiman, 2007). Indeed, the numerous shield volcanoes evident on Venus appear analogous to basaltic shield volcanoes and seamounts on Earth. Steep-sided domes have

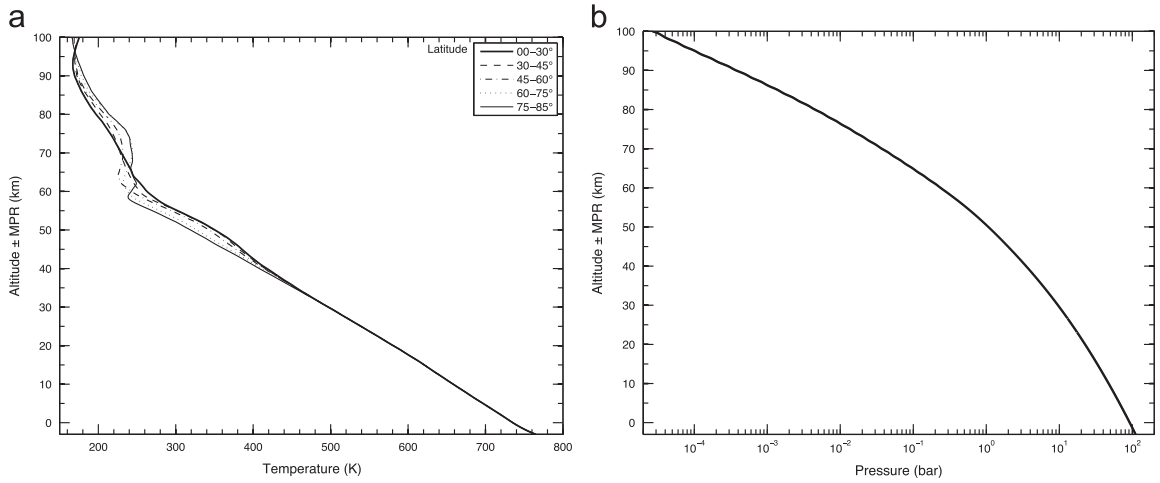

Fig. 1. Profiles through the Venus atmosphere from −3 km to 100 km relative to MPR of (a) temperature and (b) pressure. Line styles correspond to profiles representative of latitudinal ranges as given in the key. Data from Seiff et al. (1985).

Table 2
XRF and GRS analyses of the seven soil samples analysed by the Russian lander missions, all of which landed in regions composed of plains material (Treiman, 2007).

	Venera 8	*Venera 9*	*Venera 10*	*Venera 13*	*Venera 14*	*Vega 1*	*Vega 2*
wt% oxide (XRF) or ppm element (GRS)							
SiO_2	–	–	–	45.1 ± 6.0	48.7 ± 7.2	–	45.6 ± 6.4
MgO	–	–	–	11.4 ± 12.4	8.1 ± 6.6	–	11.5 ± 7.4
FeO	–	–	–	9.3 ± 4.4	8.8 ± 3.6	–	7.7 ± 2.2
CaO	–	–	–	7.1 ± 2.0	10.3 ± 2.4	–	7.5 ± 1.4
Al_2O_3	–	–	–	15.8 ± 6.0	17.9 ± 5.2	–	16.0 ± 3.6
TiO_2	–	–	–	1.6 ± 0.9	1.25 ± 0.8	–	0.2 ± 0.2
MnO	–	–	–	0.2 ± 0.2	0.16 ± 0.16	–	0.14 ± 0.24
K_2O	–	–	–	4.0 ± 1.2	0.2 ± 0.14	–	0.1 ± 0.16
Na_2O	–	–	–	n.d.	n.d.	–	n.d.
K	40,000 ± 24,000	4700 ± 1600	3000 ± 3200	–	–	4500 ± 4400	4000 ± 4000
U	2.2 ± 2.4	0.60 ± 0.32	0.46 ± 0.52	–	–	0.64 ± 0.94	0.68 ± 0.76
Th	6.5 ± 0.4	3.65 ± 0.48	0.70 ± 0.74	–	–	1.5 ± 2.4	2.0 ± 2.0

been cited as evidence for a more felsic composition (Pavri et al., 1992) but this is controversial and an evolved basaltic source has been proposed instead (Stofan et al., 2000).

The concentration of the main volatile phases within the ascending magma are also very important when simulating eruptions since it has a very strong control on magma explosivity and the resulting exit velocity at the vent (Wilson et al., 1980). In contrast to terrestrial studies, in which the magmatic volatiles are known to be predominantly H_2O, Venus is thought to have a drier mantle (Nimmo and McKenzie, 1998) in which the planetary inventory of H_2O was outgassed and incorporated into the thick clouds or broken down by UV photodissociation and lost to space from the upper atmosphere (De Bergh et al., 1991; Donahue et al., 1982; Donahue, 1999; Grinspoon, 1993). Therefore, the more prominent role of magmatic CO_2 is explored here, in addition to H_2O. H_2O, however is the chief volatile modelled here, not least because it is the main component observable in the lowest scale heights (up to ~25 km) on Venus (Bézard et al., 2009, 2011), and therefore a ideal target in the search for volcanic emissions at the surface.

2. Methods

2.1. Initial conditions

This study models a simulated crustal host rock and magma source of a composition similar to that at the Venera 14 site (Table 2) and comparable to terrestrial tholeiitic basalt. This appears to be the least-weathered and best analogue for typical Venusian crust and magmas. The volatile phase of the magma is modelled to contain varying contributions of H_2O and CO_2 to simulate different likely volatile scenarios, as the true contributions are unknown. To more accurately quantify conduit/plume behaviour, future work should also include SO_2 explicitly in models.

In terms of physical conditions that affect column dynamics, key parameters to consider include the density of crustal material, which determines the lithostatic pressure at depth in the crust, and the conduit geometry, which affects the pressure gradient along the depth of the conduit modelled (Wilson et al., 1980). In this study, basalt of density 2800 kg m^{-3} encloses a cylindrical conduit of a 25 m radius, constant along its length, with the exception of the results discussed in Section 3.5, which explores the effects of other conduit radii. The key property of the magma controlling explosivity is its viscosity, which is a function of composition, volume of exsolved gas, and temperature, and is simulated over the range 1200–1700 K (encompassing the range representative of typical terrestrial basaltic magmas). Crystallisation is not modelled here to simplify the model and a constant melt fraction of 100% is used in all model runs. The depth of the magma chamber influences the degree of volatile saturation at the base of the conduit, which can affect conduit processes; this study uses a conduit length of 5 km, with the exception of the results discussed in Section 3.6, which explores the effects of other conduit lengths.

2.2. Model setup

In order to simulate the processes occurring within the ascending magma, we combined a simple conduit flow code (Section 2.3) with outputs from a model for the solubility of C, O, H, S, Cl species in basaltic magmas, SolEx (Witham et al., 2012). In the original work of Witham et al. (2012), the SolEx model, based on the original code of Dixon (1997), was compared with the experimental work of Lesne et al. (2011) and was found to match experimental data reasonably well. Also in that study, the model was compared with the models of Newman and Lowenstern (2002) and Papale et al. (2006); it was found to match the former well for mid-ocean ridge basalt melts (MORB) and the latter for ocean island basalt melts (OIB). As a result, it was suggested that SolEx represented a model that could effectively simulate a wide range of basaltic compositions.

SolEx can be parameterised to run for all the initial conditions considered here and produces output covering the full range of pressures required. Therefore, using SolEx provides a thorough treatment of the degassing regimes without the need to incorporate this aspect into the conduit model. SolEx output was generated for closed-system degassing in several volatile scenarios, incorporating various contributions from H_2O and CO_2 and over a range of pressures from 0.5 to 400 MPa. These include the full range of pressures to be explored in the modelling exercise, bracketed by the lowest pressure of 4.74 MPa (atmospheric pressure at a vent 10 km above the MPR), and a pressure of ~228 MPa, being the pressure at the base of a 10 km deep conduit beneath a vent at MPR. The SolEx output variables, as a function of pressure, used in this study include the fraction of each volatile species dissolved in the magma, the total volume fraction of gas present as bubbles in the magma, and the relative contributions of each volatile species to that volume fraction.

The conduit code (Section 2.3) first of all reads in the SolEx data and interpolates all the variables to a 1 MPa resolution for use in the subsequent calculations. To specify the pressure regimes under investigation, atmospheric pressure data from the Venus International Reference Atmosphere (VIRA) (Seiff et al., 1985) dataset were used for the 0–10 km range of vent altitudes, along with Earth pressures for comparison. Pressure at depth from all these starting positions is then calculated for both Venus and Earth, assuming basaltic crust, with magma of density 2600 kg m^{-3} and corresponding values of g being 8.41 m s^{-2} for Venus and 9.81 m s^{-2} for Earth. This produces a pressure profile unique to each vent altitude. Conduit base pressures at all elevations used in the model runs are specified in Table 3. These values are higher for Earth due to the higher value of g; they are more variable on Venus however, because the more variable atmospheric component represents a more significant fraction of the lithostatic pressure at a given depth.

After defining values for the fixed model variables (Table 4), the variables unique to the scenario are specified: the elevation, the initial wt% of each volatile in the magma and the magma temperature (ranges shown in Table 4). The ranges of these inputs are simply intended to cover a representative range of scenarios. The conduit geometry is assumed circular and kept at a constant radius of 25 m and length of 5 km for the initial model runs. A constant radius of 25 m is chosen for the main study to represent a modest conduit for comparative purposes, and to reduce the necessity for an unwieldy amount of data. Although this conduit size is fairly small compared to other modelling studies that use fixed conduit radii (e.g. 40–63 m in Papale et al. (1998), 50 m in Papale and Polacci (1999)), it was chosen to be near the middle of the typical range observed for conduits on Earth (e.g. Diez, 2006; Papale and Dobran, 1994; Scandone and Malone, 1985). The magnitude of the effect of varying this property is explored in Section 3.5 and Fig. 8. Vents of this radius, or indeed the larger radii used by Papale et al. (1998), would not be visible at the Magellan radar resolution, which is sampled to 75 m pixels from an original (variable with latitude) resolution of >100 m (Ford et al., 1993). The 5 km depth to chamber is chosen to represent a standard base condition for the models and is kept constant in order to reduce the overall number of variables. This approach is similar to that of Papale et al. (1998) and Papale and Polacci (1999), where a conduit length of 7 km is used; the effect of conduit length is explored in Section 3.6. Volatile-saturated magma viscosity is calculated using the method of Giordano et al. (2008) with the Venera 14 composition and stored in a matrix from which values can be retrieved corresponding to the temperature of the magma in that run.

2.3. Model details

The core of the model is the steady-state, homogeneous flow conduit code, adapted from the previous models of Mastin and Ghiorso (2000) and Diez (2006), which were themselves based on the work of Woods (1995). In contrast to previous models that use the Runge–Kutta 4th order iterative method to solve the differential equations, this uses an iterative loop, which manually calculates (or retrieves) values for twelve properties at regular intervals from the base of the conduit to the vent and inserts them into a results matrix. The step size is set small enough (1 m) so that the solution will be equivalent to what it would have been had the Runge–Kutta method been employed. This slightly different approach enables data not generated within the code, such as the SolEx data, to be easily retrieved via a look-up table within the iterations.

First of all the depth is recorded, followed by the pressure in the mixture at that depth. This starts with the initial value for the

Table 4
Fixed values and variable ranges used in the model runs. Fixed values represent favoured values for the main study; entries in italics represent ranges explored for individual investigations in Sections 3.3–3.6.

	Fixed value	Min value	Max value
Conduit length	5 km	*4 km*	*10 km*
Conduit radius	25 m	*10 m*	*100 m*
Initial magma density	2600 kg m^{-3}		
Crustal density	2800 kg m^{-3}		
Acceleration due to gravity	8.41 m s^{-2}		
Elevation ± MPR	0 km	*0 km*	*10 km*
H_2O wt%		1%	5%
CO_2 wt%		0%	3%
Magma temperature	1200 K	*1200 K*	*1700 K*

Table 3
Conduit base pressures used in the model simulations for vent elevations up to 10 km on Earth and Venus. Values based on a magma density 2600 kg m^{-3}, g of 9.81 m s^{-2} (Earth) and 8.41 m s^{-2} (Venus), conduit length of 5 km, and atmospheric surface pressures as in Fig. 1.

Vent elev. (km)	0	1	2	3	4	5	6	7	8	9	10
Base pressure: Earth (MPa)	127.630	127.620	127.610	127.600	127.592	127.584	127.578	127.571	127.566	127.560	127.557
Base pressure: Venus (MPa)	118.540	117.975	117.439	116.931	116.450	115.995	115.565	115.158	114.774	114.411	114.069

maximum depth calculated previously (Section 2.2) along with an incremental change according to Eq. (1).

$$\frac{dp_c}{dz_c}\left(1-\frac{u_c^2}{u_s^2}\right) = -\rho_c g - \frac{\rho_c u_c^2 f}{r_c} \tag{1}$$

where dp_c is the change in pressure in the conduit, z_c is the vertical coordinate (1 m), u_c is the magma velocity, u_s is the acoustic velocity in the mixture, ρ_c is the density of the mixture, g is the acceleration due to gravity, r_c is the conduit radius, and f is a friction term. The friction term is calculated using Eq. (2). The first term represents the frictional component due to the viscosity of the magma and the second, f_0, is a constant that represents the effect of friction imposed by the roughness of the conduit walls. This constant is taken to be 0.0025, a value generally used to represent a rough walled eruptive conduit (e.g. Wilson et al., 1980).

$$f = \frac{16\eta}{\rho_c u_c D} + f_0 \tag{2}$$

where D is the conduit diameter and η is the viscosity of the gas–liquid mixture and is calculated using Eq. (3a) below the fragmentation depth (volume fraction gas ≤ 0.75) or Eq. (3b) above (volume fraction gas > 0.75).

$$\eta = \frac{\eta_m}{1-\phi} \tag{3a}$$

$$\eta = \eta_g\left(1-\left(\frac{1-\phi}{0.62}\right)\right)^{-1.56} \tag{3b}$$

where η_m is the volatile-saturated isothermal magma viscosity corresponding to the fixed model magma temperature, η_g is the gas viscosity (taken to be 5.3×10^{-5} Pa s), and φ is the volume fraction gas corresponding to the local pressure taken from SolEx.

The values of H_2O and CO_2 wt% dissolved in the magma are recorded individually and summed, and the total volume fraction of gas is recorded. From these, the mass fraction of the gas exsolved from the magma (Eq. (4)), and the mixed gas constant resulting from the various volatile components (Eq. (5)) are calculated.

$$n_c = \frac{n_{c0}-n_m}{1-n_m} \tag{4}$$

$$R_{mixed} = \left(n_{H_2O}\times R_{H_2O}\right) + \left(n_{CO_2}\times R_{CO_2}\right) \tag{5}$$

where n_c is the mass fraction of exsolved gas, n_{c0} is the original volatile content, n_m is the pressure-dependent volatile mass fraction in the magma (from SolEx), R is the gas constant for the corresponding subscript, and n_{H_2O}&n_{CO_2} are the relative contributions of the corresponding volatiles (from SolEx). Next, the mixture density and ascent velocity are calculated using Eqs. (6) and (7).

$$\frac{1}{\rho_c} = \frac{n_c R_{mixed} T_m}{p_c} + \frac{1-n_c}{\rho_m} \tag{6}$$

$$u_c = \frac{Q}{\rho_c A} \tag{7}$$

where T_m is the magma temperature, Q is the mass flux, and A is the cross-sectional area of the conduit. Q is calculated using Eq. (8).

$$Q = \rho_{c0} u_{c0} A \tag{8}$$

where ρ_{c0} is the initial magma density and u_{c0} is the starting magma velocity, being initially 1 m s^{-1}, but subsequently modified as described later. The acoustic velocity of the mixture and Mach number of the ascending magma are then calculated using Eqs. (9) and (10).

$$u_s = \sqrt{\left(\frac{R_{mixed}T_m}{n_c}\right)\left(n_c + (1-n_c)\frac{p_c}{\rho_m R_{mixed} T_m}\right)} \tag{9}$$

$$M = \frac{u_c}{u_s} \tag{10}$$

where M is the Mach number. These calculations are performed for each entry in the results matrix and the conditions at the vent are then assessed. If the pressure at the vent is equal to the atmospheric pressure, the eruption occurs at its subsonic velocity. If however sonic conditions are achieved at some point in the conduit of constant radius, meaning the flow is choked, the mixture can no longer decompress and therefore can no longer accelerate. The mixture must therefore erupt at $M=1$. If none of these conditions are met, the initial velocity is increased in diminishing increments (increasing Q) until either atmospheric pressure (subsonic eruption) or $M=1$ (choked flow) is attained. The final values are then stored in a new matrix corresponding to unique conditions of volatile regime, elevation, and magma temperature.

For the purposes of this study, scenarios that exceeded a volume fraction of 0.75 at the vent are assumed to erupt explosively as this is where the bubbly liquid regime transitions to the gas with suspended liquid droplets regime (Sparks, 1978). Caution must be exercised in applying this criterion because the fragmentation process is more complex and occurs at a range of values between 0.7 and 0.8 volume fraction gas. Factors thought to define the point of fragmentation include the point at which the gas overpressure exceeds the tensile strength of the magma, causing bubble disruption (Zhang, 1999), or when the rapid decompression causes rapid bubble growth such that the deformation rate exceeds that of the structural relaxation rate of the magma (Papale, 1999). Future modelling work to capture these relatively poorly constrained processes is to be encouraged but is beyond the scope of this study.

A subsequent test is carried out to ascertain whether or not the resulting plume achieves buoyancy. In order to do this the results of the conduit flow model are used as input to a subaerial plume dynamics model (Glaze et al., 1997), based on the work of Woods (1988) and Morton et al. (1956). This code generates values for the plume height and the neutral buoyancy height (if buoyant). When linking these models, the jet decompression to atmospheric pressure upon eruption is accounted for using a linking code based on the method of Woods and Bower (1995) as follows.

The conditions above the vent, where the pressure of the jet has decompressed sufficiently to be in equilibrium with atmospheric pressure, can be evaluated first of all by using the approximation for the jet density described in Eq. (11).

$$\rho_d \sim \frac{p_{atm}}{n_{c0} R_{mixed} T_m} \tag{11}$$

where ρ_d is the density of the decompressed jet and p_{atm} is the atmospheric pressure. The velocity resulting from jet decompression is calculated using Eq. (12).

$$u_d = (n_{c0} R_{mixed} T_m)^{0.5} \alpha\beta\left(1+\frac{n_c}{n_{c0}\alpha\beta^2}\left(1-\frac{p_{atm}}{p_c}\right)\right) \tag{12}$$

where u_d is the velocity of the decompressed jet and

$$\alpha = 1 + \frac{(1-n_c)p_c}{n_c R_{mixed} T_m \rho_m} \tag{13}$$

$$\beta = \frac{n_{c0}-n_m}{n_{c0}^{0.5}\left(n_{c0}-\frac{n_m}{2}\left(1+\frac{p_c}{R_{mixed}T_m\rho_m}\right)\right)^{0.5}} \tag{14}$$

Using these newly calculated variables, the physical dimensions of the jet can then be calculated using Eqs. (15) and (16).

$$A_d = \frac{Q}{u_d \rho_d} \tag{15}$$

$$r_d = \left(\frac{A_d}{\pi}\right)^{0.5} \tag{16}$$

where A_d and r_d are the new values for the cross-sectional area and radius of the decompressed jet.

The output from this intermediate model, where all parameters correspond to the fully decompressed jet, is then used with the original subaerial plume model of Glaze et al. (1997). The plume model details are not reproduced here for clarity, but are described exhaustively in the cited article. Parameter regions where buoyant plumes occur, and the volume fraction gas values, are mapped onto the conduit exit velocity datasets to identify up to three distinct regions of volcanic styles: effusive, explosive collapsing, and explosive buoyant.

3. Results

3.1. Model testing and validation

In order to validate the conduit flow code, a series of comparison runs were performed with the existing conduit flow code of Mastin and Ghiorso (2000), Conflow version 1.0.5. Although these codes under comparison were based fundamentally on the same constitutive relationships and governing equations, the effects of the differing approach taken with the degassing calculations (i.e. SolEx vs. that hard-coded into the Mastin model) are explored in this comparative analysis. Pure H_2O was modelled as the volatile phase (Conflow is not capable of simulating CO_2) from a 5 km deep, 25 m radius conduit/vent under Venusian surface conditions at MPR with magma of 1200 K temperature and a base pressure of 118.54 MPa. Fig. 2a–e show the profiles for pressure, volume fraction gas, Mach number, and velocity from each of the two models for H_2O concentrations of 1, 2, 3, 4, and 5%, respectively. The plots also show the final value of each property, describing conditions simulated at the vent.

The two models show a good overall match. This is true in particular in terms of pressure, which it is the primary aim of the conduit model to predict. The disparity between the two sets of results in the case of the volume fraction gas, and the resultant velocity, is due largely to differences between SolEx and the degassing calculations employed in Conflow. In contrast to SolEx, which uses the calculations of Dixon (1997) to quantify the melt/vapour partitioning of volatiles, Conflow uses the MELTS method of Ghiorso and Sack (1995) to calculate the chemical potential of water in the melt and the method of Haar et al. (1984) to calculate the chemical potential of water in the vapour phase. The mass fraction of water in the melt is then adjusted until the chemical potential is the same as that of the H_2O vapour.

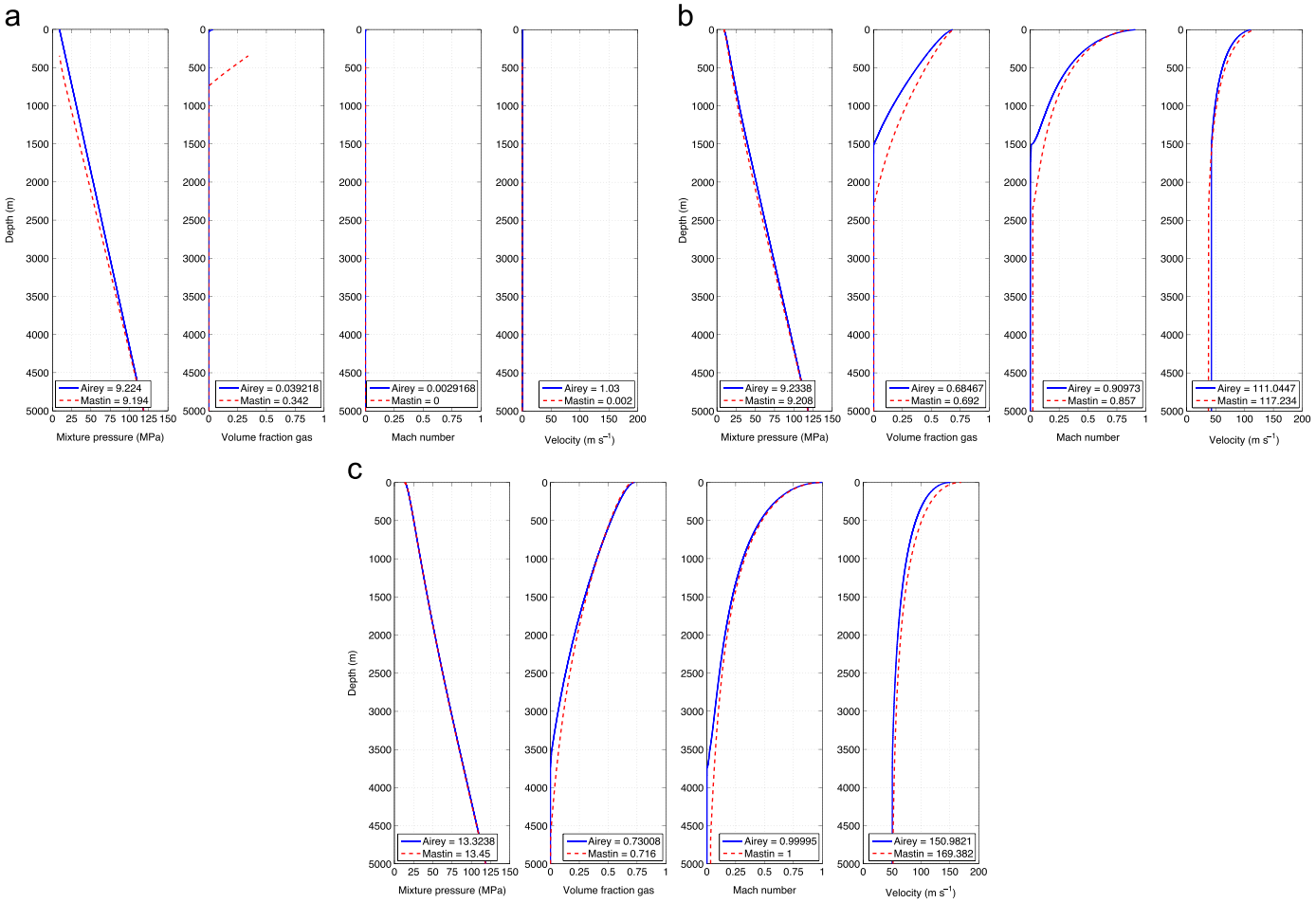

Fig. 2. Conduit flow model comparisons between the existing model of Mastin and Ghiorso (2000) (red, dashed curves) and the model developed in the current study (blue, solid curves) for (a) 1% H_2O, (b) 2% H_2O, (c) 3% H_2O, (d) 4% H_2O and (e) 5% H_2O. The values of pressure, volume fraction gas, Mach number, and velocity stated in the key represent the final value recorded at the vent (i.e. depth=0 m). (For interpretation of the references to color in this figure legend, the reader is referred to the web version of this article.)

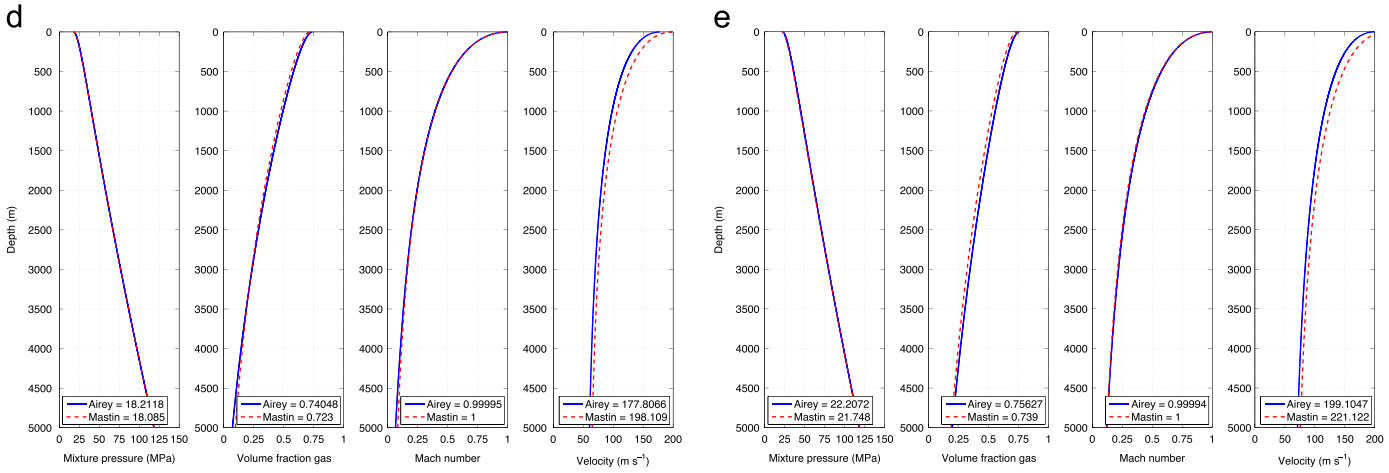

Fig. 2. (*continued*)

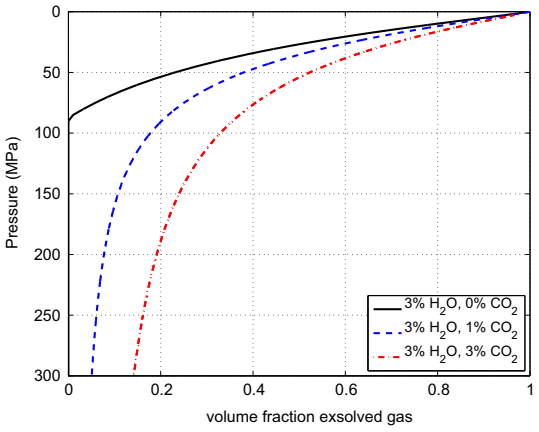

Fig. 3. Volume fraction exsolved gas in a basaltic magma as a function of confining pressure for various initial volatile concentrations, from 3 wt% H_2O to 3 wt% H_2O+3 wt% CO_2.

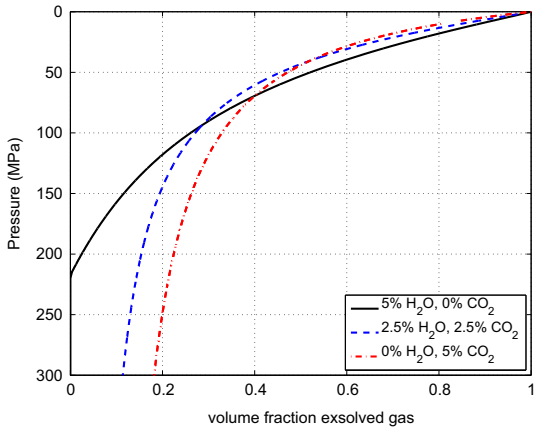

Fig. 4. Volume fraction exsolved gas in a basaltic magma as a function of confining pressure for a constant initial volatile content of 5% with varying contributions from H_2O and CO_2 as shown in the key.

In order to also include CO_2, we modelled an H_2O/CO_2 volatile mix in SolEx, and adapted the gas constants as appropriate in the calculations. To explore the effect of this mixed volatile phase, we modelled the degassing of basalt at a temperature of 1200 K with varying volatile inventories in SolEx. Fig. 3 shows the results when keeping the H_2O content fixed (3%) and calculating the effect of increasing the CO_2 composition from 0 to 3%. As expected, the increase in CO_2 (along with the increase in total volatile content) results in deeper onset of degassing, due to the much lower solubility of CO_2, and a higher total volume fraction at all pressures until 0 MPa. When the substitution of H_2O with CO_2 is considered (Fig. 4), the trend at high pressures shows an increase in the volume fraction gas with increasing CO_2 contribution as expected. However, at lower pressures the curves intersect resulting in an inversion in the trend of the degree of exsolution i.e. at a given pressure, say 25 MPa, an increase in the contribution from CO_2 results in a decrease in the volume fraction of gas. This could partly be due to the use of the model beyond its calibrated range for CO_2, as only examples of <1 wt% CO_2 are explored/compared with experimental data in the original work of Witham et al. (2012) and therefore results for high-CO_2 runs are considered with caution.

3.2. Effect of CO_2 addition on volatile exsolution and velocity

Fig. 5a and b shows the modelled conditions at the vent on both Earth and Venus when the H_2O concentration of a magma is kept constant (3%), but the CO_2 concentration is varied. The models were run for a 5 km long, 25 m radius conduit with magma temperature 1200 K and base pressures of 127.63 MPa (Earth) or 118.54 MPa (Venus). As the final pressure at the vent increases with the initial additional CO_2, so does the exit velocity. Where CO_2 concentration is $>1\%$ on Earth and $>0.5\%$ on Venus the volume fraction of exsolved gas also increases with addition of CO_2. Below these thresholds however, there is an initial drop in volume fraction of exsolved gas with the introduction of CO_2 to the magma. The increase in initial magmatic CO_2 content alters the pressure gradient within the conduit resulting in a higher magmatic pressure at any given point in the conduit (shown in Fig. 5 for the surface). The result of this is a greater proportion of the gas phase being stable dissolved in the magma up to a point (1% on Earth, 0.5% on Venus in this example), after which further addition increases the degree of total gas exsolution. This change occurs as a greater volume of total volatile is present and the effect of increased gas volume outweighs that of the increased pressure. On Earth, the effect on volatile exsolution of adding CO_2 does not return the volume fraction gas to values greater than the original, pre-CO_2 value when modelled up to an additional 3%. On Venus however, once $>\sim 2\%$ additional CO_2 has been added, the volume of exsolved gas exceeds the original pre-CO_2 value.

3.3. Effect of variations in elevation

The decrease in atmospheric pressure with elevation on Venus can be seen in Fig. 1. This has an effect on conduit processes, as the

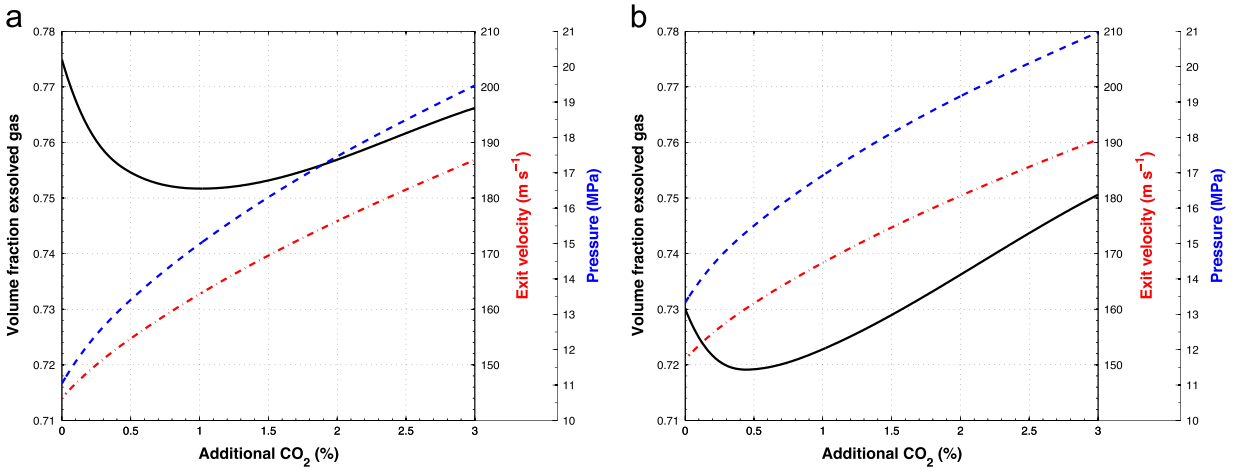

Fig. 5. The response of volume fraction gas (black, solid curves), exit velocity (red, dot–dash curves), and pressure (blue, dashed curves) to an increasing concentration of CO_2 (0–3%) added to magma of constant H_2O concentration (3%). Values correspond to conditions at the volcanic vent of radius 25 m above a conduit of 5 km length, and a magmatic temperature of 1200 K at (a) Earth's surface and (b) Venus' MPR. Base pressures are 127.63 MPa (Earth) or 118.54 MPa (Venus). (For interpretation of the references to color in this figure legend, the reader is referred to the web version of this article.)

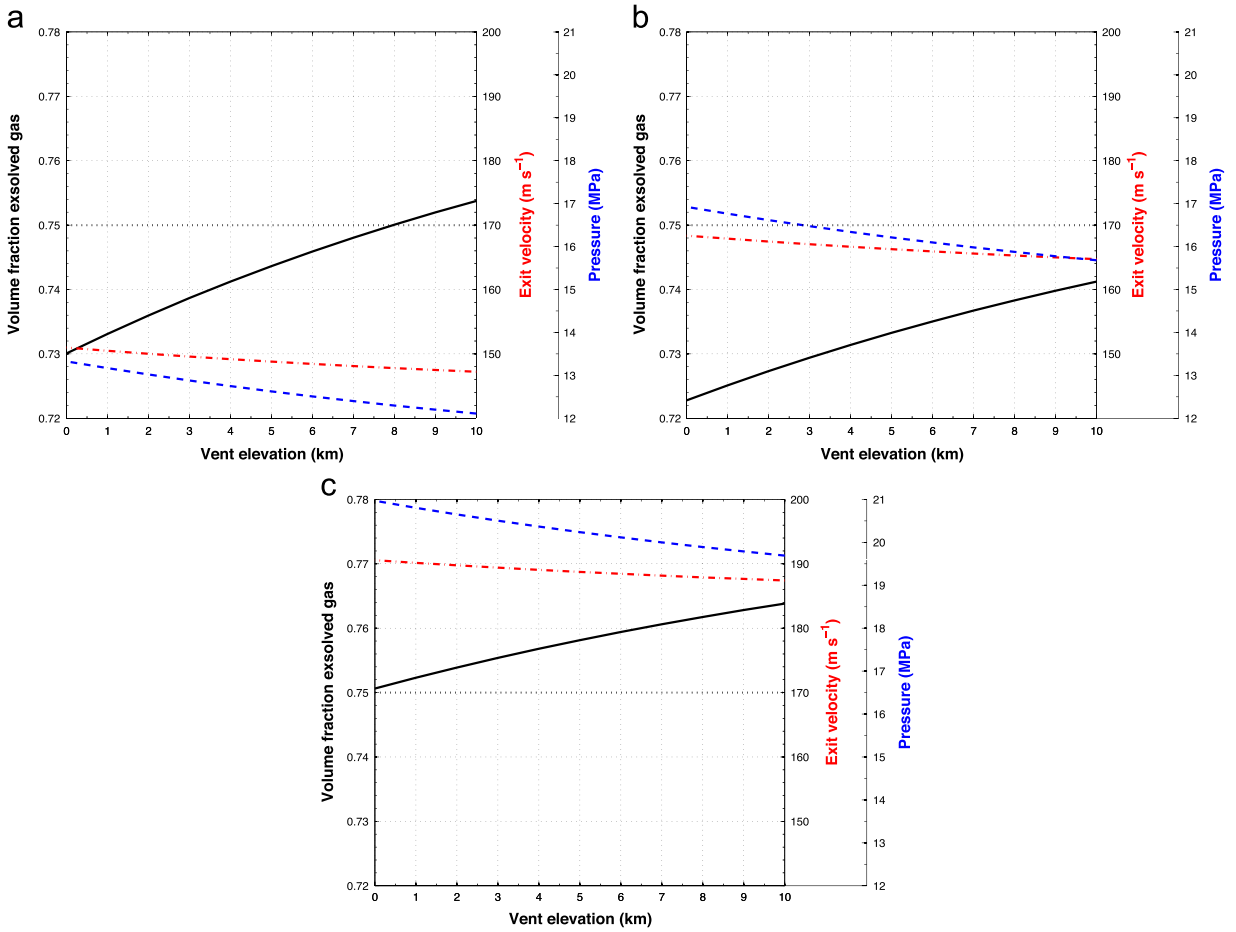

Fig. 6. Effects of elevation on volume fraction gas (black, solid curves), exit velocity (red, dot–dash curves), and vent pressure (blue, dashed curves) at a 25 m radius volcanic conduit on Venus with a basaltic magma of 1200 K, 3% H_2O, and an additional (a) 0%, (b) 1%, and (c) 3% CO_2. The horizontal dotted line corresponds to the estimated fragmentation criterion. Base pressures as in Table 3. (For interpretation of the references to color in this figure legend, the reader is referred to the web version of this article.)

confining environment is less extreme and therefore the lithostatic pressure at the base of the conduit is lower for higher elevation vents. Model runs were simulated for elevations up to 10 km above MPR to recreate the range of volcanic vent incidences observed on Venus. These were again run with a conduit of 5 km length and 25 m radius, a magma temperature of 1200 K, and base pressures as in Table 3. The same scenarios used in Fig. 5 were used to explore the effects of elevation on vent pressure, velocity, and volatile exsolution. Results of three examples of volatile combinations (3% H_2O with 0%, 1%, and 3% additional CO_2) are shown in Fig. 6. An increase in vent pressure and exit velocity with CO_2 addition is observed, as is the drop/rise in volume fraction gas

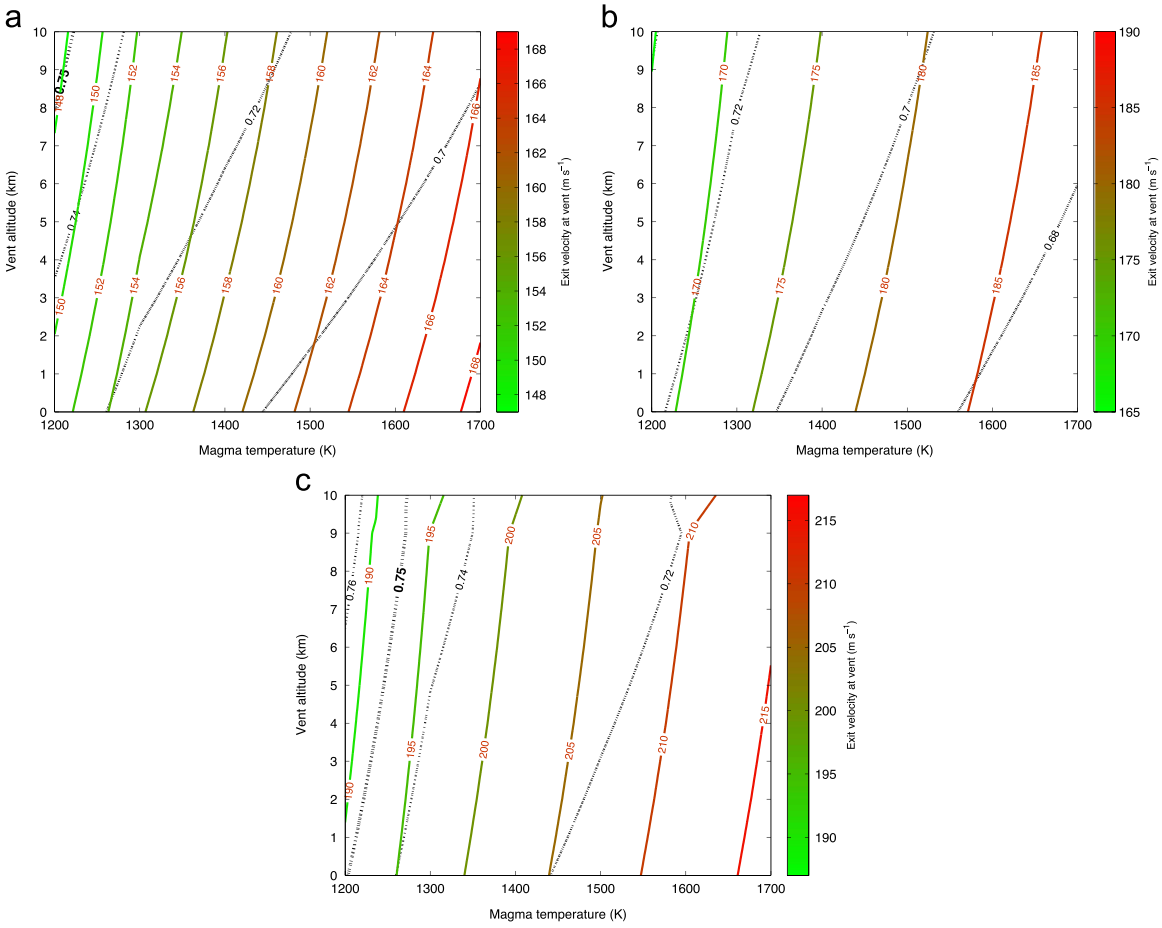

Fig. 7. Volume fraction gas (black, dashed contours) and exit velocity (coloured, solid contours) as a function of vent altitude and magma temperature. The fragmentation threshold, volume fraction gas=0.75, is highlighted in bold. Models run for a basaltic magma emerging from a 5 km deep, 25 m radius conduit with 3% H_2O and an additional (a) 0%, (b) 1%, and (c) 3% CO_2. Base pressures as in Table 3. (For interpretation of the references to color in this figure legend, the reader is referred to the web version of this article.)

seen in the previous section. The effect of increasing altitude is to decrease the vent pressure and increase the volume fraction of gas in the magma. This is due to the decrease in lithostatic pressure at any given depth in the conduit, allowing more of the volatile phase to be stable as gas bubbles in the magma. The actual fall in vent pressure with altitude is less than the fall in surface atmospheric pressure with vent altitude, $\sim 1.2 \times 10^5$ Pa km^{-1} in contrast to $\sim 4.5 \times 10^5$ Pa km^{-1}, an effect of the flows being choked and therefore unable to fully decompress. The effect on velocity of increasing altitude is almost negligible. This is because, as the eruptions are all choked in these examples, they erupt at their sonic velocity. The sonic velocity decreases only very slightly with decreasing pressure, and therefore increasing altitude, by ~ 0.3 m s^{-1} km^{-1}. As these model runs were all simulated at an isothermal 1200 K, the dependency of sonic velocity on temperature is not represented in these results.

3.4. Effect of variations in magma temperature

So far all model runs have been conducted at the conservative temperature, in terms of typical terrestrial basaltic eruptions, of 1200 K in order to compare the effects of other variables. If however, the effect of hotter magmas within a reasonable range based on terrestrial temperatures is considered, further effects on magma properties at the vent become apparent. Fig. 7 introduces this new variable into the existing model examples, being representative of magmas containing 3% H_2O with 0%, 1%, and 3% CO_2, respectively. These simulations were again run with conduits of 5 km length and 25 m radius, and base pressures as in Table 3. It is apparent that, at any given altitude, an increase in magma temperature results in an increase in exit velocity and a decrease in volume fraction gas. The increased temperature reduces the viscosity of the magma allowing higher velocities to be attained due to reduced friction with the conduit walls. The effect of this, however, is to reduce the magnitude of the drop in pressure with ascent resulting in a higher pressure at the vent and a correspondingly lower degree of volatile exsolution.

3.5. Effect of variation in conduit radius

The geometry of the conduit through which the ascending magma propagates is another important factor to consider. Thus far, the conduit geometry used in all model runs has been a perfect cylindrical tube of a constant 25 m radius. In reality a great range of sizes can occur. Although linear geometries are not considered here, the effects of varying the size of a cylindrical conduit are explored in Fig. 8. When maintaining constant magma temperature, elevation, and volatile composition/concentration (1200 K, MPR, 118.54 MPa base pressure, 3% H_2O, 0% CO_2), it is clear that circular conduits of a larger cross sectional area favour higher velocities (as increasing D reduces the friction term in Eq. (2)), and less volatile exsolution due to the higher conduit pressure. Up to $\sim$50 m radius, even small variations in conduit size can be seen to have pronounced effects on these properties. At radii over 50–100 m, the magnitude of the effect of increasing the conduit size

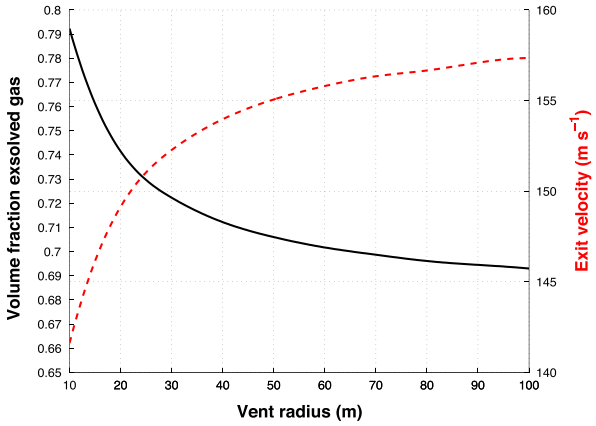

Fig. 8. Volume fraction exsolved gas (black, solid curve) and exit velocity (red, dashed curve) as a function of conduit radius for a basaltic magma erupting at Venus' MPR with a 5 km long conduit, 3% H_2O, a magma temperature of 1200 K, and a base pressure of 118.54 MPa. (For interpretation of the references to color in this figure legend, the reader is referred to the web version of this article.)

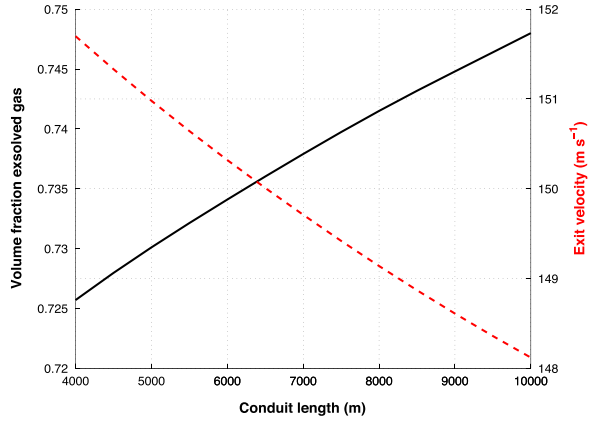

Fig. 9. Volume fraction exsolved gas (black, solid curve) and exit velocity (red, dashed curve) as a function of conduit length for a basaltic magma erupting at Venus' MPR with a conduit of radius 25 m, 3% H_2O, and a magma temperature of 1200 K. (For interpretation of the references to color in this figure legend, the reader is referred to the web version of this article.)

decreases, eventually approaching an asymptotic value corresponding to the individual scenario conditions.

3.6. Effect of conduit length

The bulk of this study considers a constant conduit length of 5 km, however varying the conduit length in these simulations affects the results as described in Fig. 9. Base pressures range from ~97 MPa at 4 km long conduits to ~229 MPa for 10 km long conduits. Simulations are run at 3% H_2O, 25 m conduit radius and 1200 K magma temperature. Longer conduits result in lower velocities but have only a very minor effect, <4 m s^{-1} with an increase in depth of 6 km. The effect on volatile exsolution, however, is more prominent. Increasing the conduit length alters the pressure gradient such that deeper chambers result in a lower conduit pressure immediately prior to eruption, increasing the degree of exsolution and the likelihood of fragmentation within the conduit.

3.7. Jet decompression of choked flows at the vent

Upon eruption at the surface, an overpressured choked flow will rapidly decompress to atmospheric pressure resulting in an increase in the eruption column velocity and radius. Figs. 10 and 11 show the effect of jet decompression on velocity and column radius, respectively, as a function of volatile content, above the vent. The contrast between a given conduit pressure and atmospheric pressure is much more pronounced on Earth than it is on Venus as a result of the much higher atmospheric pressure on Venus. The examples shown in Figs. 10 and 11 are for jets emerging at the MPR from a 5 km long conduit of 25 m radius with magma of Venera 14 composition (Table 2), a temperature of 1200 K, and base pressures of 127.63 MPa (Earth) or 118.54 MPa (Venus).

The changes to jet variables caused by decompression on Earth can clearly have an important influence on plume behaviour. Considering a magmatic H_2O range of 1–5% (Figs. 10a and 11a) and the initial conditions specified above, an increase in velocity of ~70% and an increase in column radius to ~4–10 times the initial value can occur. When using these results in column buoyancy modelling, jet decompression is therefore an important process to consider. When adding CO_2 to a scenario with a constant magmatic H_2O concentration of 3% (Figs. 10b and 11b), the effect is similar, but rather less pronounced.

When the above conditions are applied to Venus it is found that the effects are subtler, with a velocity increase of up to ~35% between 2 and 5% H_2O (eruptions with $<2\%$ H_2O erupting subsonically), and a column radius increasing by only a few metres (Figs. 10a and 11a). As with the terrestrial example, adding CO_2 to a base value of 3% H_2O has a small but significant effect on these column properties (Figs. 10b and 11b). The velocity with an increase of up to ~35% when given a large additional input of CO_2, and the radius increase being negligible. These results for Venus are only applicable as input to the plume buoyancy model, under these base conditions, to H_2O concentrations $>4.5\%$ (Figs. 10a and 11a) and $H_2O=3\%$ with $>3\%$ additional CO_2 (Figs. 10b and 11b) i.e. where the volume fraction gas exceeds 0.75. Below these thresholds, the jets would collapse following decompression regardless, as the unfragmented material cannot undergo the column buoyancy processes involving atmospheric entrainment described in Section 1.1.

4. Discussion

4.1. Explosivity of eruptions

A great many factors influence the behaviour of volcanic events. As discussed above, the potential for explosive volcanic activity on Venus is often discounted because of the high atmospheric pressure compared with Earth. Adopting the method of a critical threshold for magmatic fragmentation, here assumed to be a volume fraction of 0.75 gas in the magmatic mixture (Sparks, 1978), our modelling suggests that there are certain scenarios in which explosive volcanism is feasible on Venus. As discussed above, fragmentation processes are more complex and occur at a range of values between 0.7 and 0.8 volume fraction gas and are also influenced by other factors such as the tensile strength of the magma and the structural relaxation rate of the magma (Papale, 1999; Zhang, 1999).

One of the major considerations when investigating whether or not explosive volcanism may occur is the requirement in terms of the initial concentration of volatiles in the magma. As discussed above, the interior of Venus may well be considerably drier than Earth's and so it is worth considering the effect of lower H_2O concentrations and the role of CO_2. On its own, CO_2 as the primary volatile phase cannot be responsible for explosive volcanism. Model runs with pure CO_2 have demonstrated that a magma of 1200 K emerging from a 25 m radius conduit would require a CO_2 concentration in excess of ~6.5% at an altitude of 10 km above MPR, or ~7.5% at the MPR in order to achieve the fragmentation. However, it is probable that minor volatile phases such as CO_2

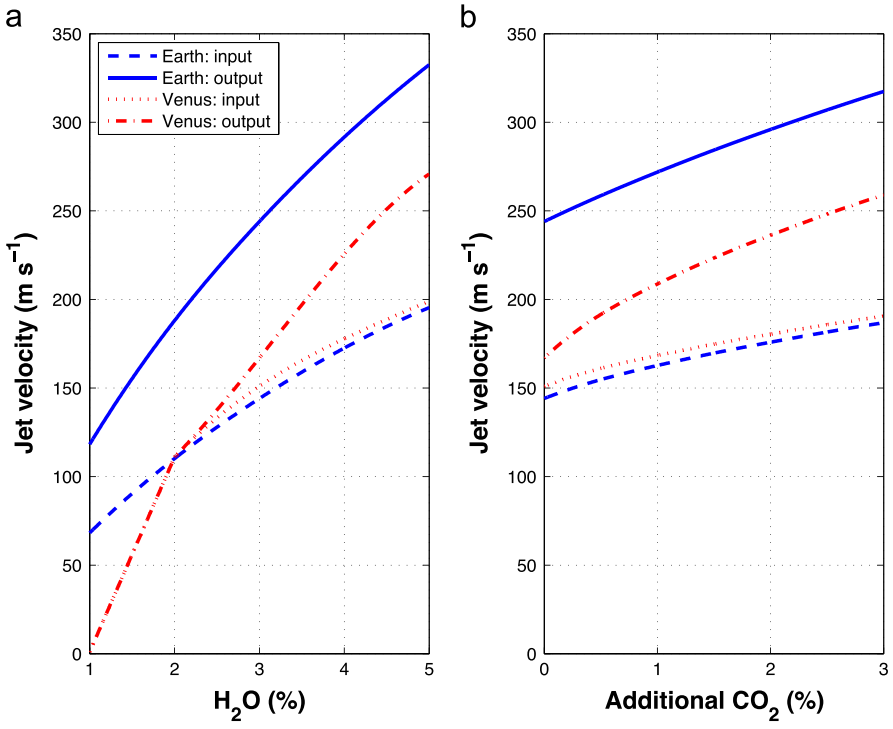

Fig. 10. The effect of jet decompression on jet velocity from a 5 km long conduit of radius 25 m with magma of Venera 14 composition, magma temperature of 1200 K, base pressures of 127.63 MPa (Earth) or 118.54 MPa (Venus), and (a) H_2O concentrations from 1 to 5%, or (b) CO_2 concentrations up to 3% added to a constant H_2O concentration of 3%. Results are compared for Earth and Venus as described in the key; 'input' data correspond to the initial velocity at the vent immediately upon eruption and 'output' data correspond to the final velocity when the jet has decompressed to local atmospheric pressure.

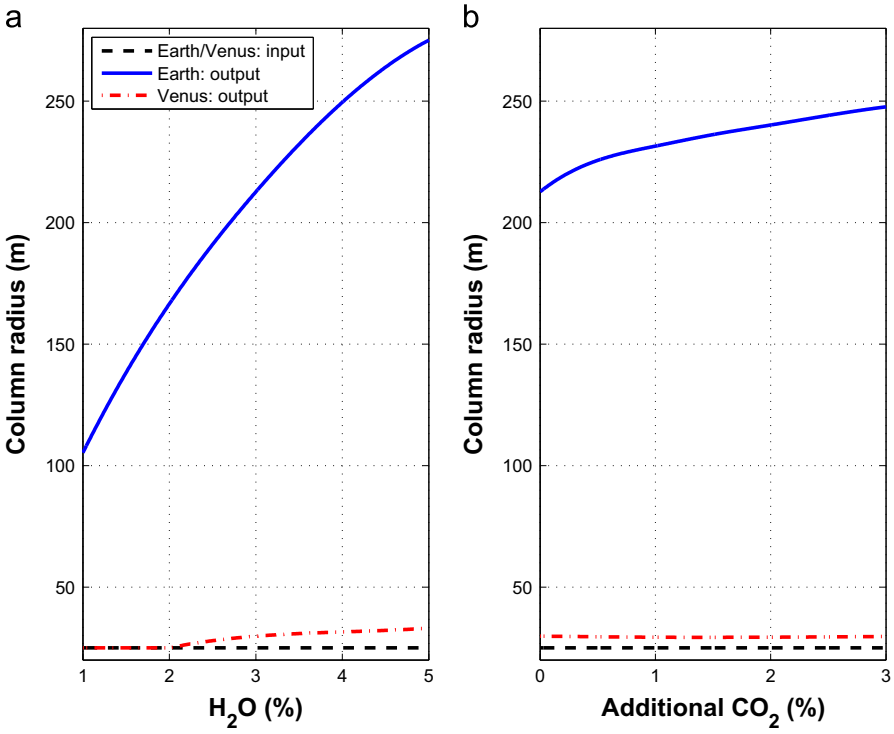

Fig. 11. The effect of jet decompression on eruption column radius from a 5 km long conduit of radius 25 m with magma of Venera 14 composition, magma temperature of 1200 K, base pressures of 127.63 MPa (Earth) or 118.54 MPa (Venus), and (a) H_2O concentrations from 1 to 5%, or (b) CO_2 concentrations up to 3% added to a constant H_2O concentration of 3%. Results are compared for Earth and Venus as described in the key; 'input' data correspond to the initial column radius immediately upon eruption, i.e. the vent radius of 25 m in all cases on both Earth and Venus, and 'output' data correspond to the final column radius when the jet has decompressed to local atmospheric pressure.

contribute to the volatile inventory, thereby reducing the total H_2O requirement for explosive volcanism to occur. If this is the case, accessory volatiles are likely to be required in much higher concentrations, i.e. $>1\%$, than are commonly found on Earth. Although plate tectonics is apparently absent on Venus, it is likely that a wide variety of melt source regions occur on Venus through

other tectonic and fractionation processes, and that these may concentrate volatile rich material.

Although this might suggest that sufficient CO_2 as a primary volatile is unlikely, other mechanisms could result in this volatile causing explosive behaviour. For example, as the atmosphere of Venus is a supercritical fluid, it could potentially circulate through the upper crust and gather in fluid-rich pockets that could violently mix with ascending magma resulting in an explosive response. Alternatively, degassing of a stalled magma body may cause the build up of pressure and transient vulcanian activity (Fagents and Wilson, 1995).

Our modelling shows that if explosive volcanism does occur, H_2O is very likely required in magmatic systems. Evidence in support of excess H_2O in the mantle includes the possibility of re-fertilisation of the mantle with volatiles due to gravitational instabilities at the base of the lithosphere (Elkins-Tanton et al., 2007) and in contrast to the D/H ratio, atmospheric Ar measurements indicate that as little as 25% of the planetary inventory of H_2O might have been outgassed from the interior (Kaula, 1999).

The Venus models presented here are based entirely on the most representative geochemical analysis available, the Venera 14 lander, which appears to have detected a tholeiitic-type basalt. No felsic material has been measured so far by direct measurement, and using alternative lander data would only vary the model results little. It is widely assumed that the vast majority of volcanic rocks on Venus are basaltic based on this, and on radar observations of lava flow morphology. This may indeed be the case but regions with a more felsic composition are certainly plausible and are inherently more likely to produce explosive behaviour because of their higher silica content and viscosity. The 1 μm emissivity data retrieved by VIRTIS (Visible and Infrared Thermal Imaging Spectrometer on Venus Express) and processed by Mueller et al. (2008) shows consistently low emissivity returns from tessera regions (deformed highland terrains) and is interpreted as more felsic material due to the lower emissivity of felsic minerals (e.g. quartz, feldspars) at this wavelength. Pavri et al. (1992) suggest that the steep-sided-domes seen on Venus could be the result of more felsic eruptions based on their inferred flow rheology. Geochemical modelling shows that more felsic source regions could be created as a result of fractional crystallisation of rocks of Venera compositions (Shellnutt, 2013) in the presence of H_2O.

When modelling the effect of composition on magmatic processes, the effect of crystallisation should also be considered. In this work, a constant melt fraction of 100% is assumed. If, however, crystallisation did occur during magma ascent, the composition would vary as a function of melt fraction and volatiles would preferentially partition into the melt, thereby promoting bubble growth such that the volume fraction of gas in the conduit, and the viscosity, would increase (Gonnermann and Manga, 2012). Both of these processes increase the potential explosivity of the magma and, as a result, our values of requirements for fragmentation represent upper estimates.

Temperature also has an effect on viscosity. Fig. 7 shows that by increasing the temperature, and therefore reducing the viscosity, the volume of exsolved gas attainable in the mixture is reduced. Cooler, more gas-rich, magmas therefore favour explosivity. In the absence of any data to the contrary, it is assumed that eruptions on Venus erupt at similar temperatures to their terrestrial counterparts i.e. bracketed by the range of temperatures modelled in Fig. 7 for basaltic eruptions.

It is likely that a wide variety of conduit geometries will occur on Venus. The Magellan radar data are not of sufficient resolution to show volcanic vents in fine detail, but the evidence for shield volcanoes of a vast range of sizes and large areas of rifting indicate a corresponding array of potential conduit geometries. All else being equal, these model results show that smaller vents, overlying smaller radius conduits, perhaps occurring as individual volcanoes in larger shield fields or in larger volcanic complexes, could theoretically produce localised explosive activity whereas larger examples would not.

The natural variation in conduit geometry is further complicated in that the perfect cylinder used in this study, although convenient for comparative purposes, is very unlikely to occur in nature. The conduit itself must transition from the geometries of magma source reservoir to dike to quasi-circular cross-sectional conduit. The complexities of modelling this are beyond the scope of this study, but represent an interesting challenge for future work. Transitional geometry such as this notwithstanding, the work presented here provides a first-order suite of results based on these simplified assumptions.

Another complication with regards to the conduit geometry is that this study uses a steady-state approach with no treatment of an evolving conduit structure, i.e. a flaring of the conduit from parallel-sided to cone-shaped near the surface with time, due to abrasion and conduit wall collapse. The current work is most representative of the early stages of an eruption prior to the onset of this type of temporal conduit evolution. Over time, if conduit flaring occurs, the choking depth could migrate down the conduit, creating a solution more like that of a lithostatically pressure-balanced system, potentially resulting in the onset of supersonic flow below the surface (Mitchell, 2005). Therefore, this work inherits a somewhat restricted range of possible exit velocities (either subsonic or choked). As a consequence, ongoing and long-term processes interpreted from this model should be considered with some degree of caution.

The effect of increasing altitude and the corresponding decrease of pressure in the conduit has a significant effect on generating conditions suitable for explosive volcanism. It is clear that the tops of Venus' highest peaks could host explosive vents at volatile concentrations considerably lower than those at the MPR. Volcanic peaks reaching up to ~9 km occur on Venus and Fig. 6 shows that, with the same volatile composition, volume fractions of gas could be ~2% higher (Fig. 6a) at that altitude. This effect is greater on H_2O than CO_2 as apparent from the shallowing of the volume fraction gas curves on Fig. 6.

From the preceding discussion, we can conclude that, under the right conditions, certain regions of Venus could generate explosive volcanic activity. For example a small conduit, say 30 m in diameter, with a relatively cool magma of ~1200 K and 3% H_2O could achieve conditions comfortably within those favouring explosive activity, even at the MPR (Fig. 8). It is clear that very high volatile contents are not necessarily required and explosive behaviour may be more widespread than initially thought.

4.2. Column buoyancy

Following discussion of whether explosive activity is possible, we next explore how these volcanic products would behave upon eruption. Using the output from the conduit and jet decompression models described here, subaerial behaviour in some example scenarios was simulated using a previously developed plume rise model (Glaze et al., 1997, 2011; Glaze, 1999). These example results are explored and described using the following case studies in Sections 4.3 and 4.4. It is known from previous work (Sparks, 1986; Valentine and Wohletz, 1989; Wilson et al., 1978; Woods, 1988, 1995; and others), and confirmed in these model runs, that faster, hotter eruptions are more likely to achieve buoyancy by providing greater momentum and heating of entrained air with corresponding reduction in density. In addition to this, upon eruption of a choked flow, the emitted material rapidly decompresses to atmospheric conditions, resulting in an increased velocity and radius. This decompression process is less pronounced on Venus than it is on Earth for a given exit pressure (Figs. 10 and 11) as the atmospheric pressure on

Venus is almost two orders of magnitude higher. Nonetheless, this component of the eruption process may have an effect on whether or not a buoyant regime is attained and so is duly considered.

4.3. Scathach Fluctus

If, for illustrative purposes, we use Scathach Fluctus as a potential example of a site of explosive volcanism occurring at Venus' MPR, it allows us to explore initial constraints on eruptive conditions, should an event of this nature this occur. A full description of the deposit is provided in Ghail and Wilson (2013). Assuming this eruption occurred at 1200 K, from a vent at a similar elevation to the deposit itself and of radius 25 m, in order for it to behave explosively, the model shows there must have been an H_2O content of over 4.5% (which erupts at a volume fraction of 0.749, between Fig. 2d and e). This volatile composition is not implausible based on H_2O concentrations of terrestrial magmas, although more characteristic of subduction zone settings (Wallace, 2005), and it is necessarily based on numerous assumptions. If, for example, the conduit was smaller, the vent was higher, or indeed both, the volatile requirement would be reduced accordingly (e.g. moving to the right in Fig. 6a or to the left in Fig. 8 increases the volume of exsolved gas). In addition to this, the result is based on the assumption that the composition of the magma responsible for the formation of Scathach Fluctus is the same as that at the Venera 14 site, although it remains possible that it was a more felsic source. With a lower initial H_2O concentration, explosive activity could potentially occur here given a sufficient concentration of an accessory volatile. When modelled with only 3% H_2O, it is found that close to an additional 3% of CO_2 would be required to initiate magma fragmentation, a total volatile content approaching 6% (Fig. 5, where the volume fraction exsolved gas exceeds 0.75 with 3% H_2O and an additional 3% CO_2). Again, if this was the case, it seems likely that the eruption occurred through one or smaller conduits, perhaps as part of a fissure system, as smaller conduits have lower volatile requirements in order to generate explosive eruptions (Fig. 8).

Here it has been assumed that, as the deposit is interpreted as a gravity-driven flow, the style of eruption was that of a collapsing column, i.e. explosive at the vent but not sufficiently buoyant to achieve plume rise. Indeed, within the limits of the model, it was not possible to achieve a buoyant column from a 25 m radius conduit, even with H_2O modelled up to 10%. This is also partly because increasing the modelled magma temperature to promote buoyancy also reduces the volume fraction gas achievable at a given elevation. When increasing temperature, a regime is rapidly approached where column buoyancy is simply not possible (Fig. 7).

4.4. Ma'at Mons

The next case study represents the extreme of elevation. Ma'at Mons is located at 0.5°N, 194.5°E and is the highest volcanic peak on Venus at ~9 km above MPR. No explosive deposits have been identified based on radar data, however if pressure, and by inference altitude, is thought to be the dominant property preventing explosivity it is instructive to explore how this environment contrasts with localities close to MPR such as Scathach Fluctus. Given the same parameters imposed in the previous case study (1200 K, 25 m radius), the H_2O concentration required is only ~2% (erupting with a volume fraction of 0.749, Fig. 12), less than half that required only 9 km lower. It is therefore highly probable that explosive activity can occur at higher elevations on Venus, especially so if the conduits are longer (Fig. 9). A temperature of 1200 K was only capable of producing buoyant column rise with an H_2O concentration of >6.8% (reaching ~18 km above the vent) or a mixed volatile

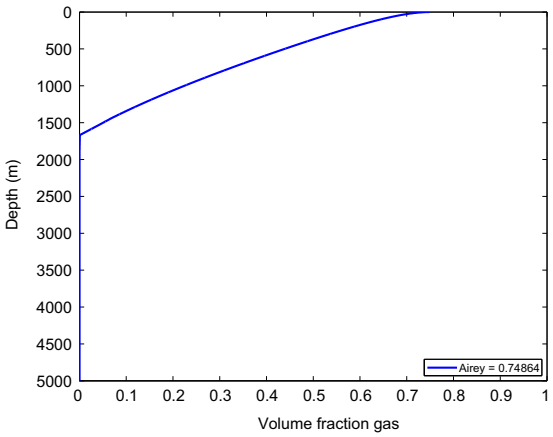

Fig. 12. Model results of the response in terms of volume fraction of gas of the exsolution of volatiles in a basaltic magma of temperature 1200 K with 2% H_2O rising through a 5 km long, 25 m radius conduit to a vent of altitude 9 km. The value in the key is the final volume fraction H_2O of the mixture at the vent. Pressure at the conduit base is 114.41 MPa (Table 3).

concentration of 3% H_2O with 3% CO_2 (reaching ~20 km above the vent). However, with a temperature of 1300 K, a buoyant volcanic column reaching ~20 km above the vent could be generated with a much more attainable H_2O concentration of >4.7%. Although higher temperatures favour buoyancy in an explosive eruption column, they also reduce the likelihood of fragmentation in the conduit. This results in a very narrow range of temperatures allowing buoyant columns to form with relatively low volatile contents, as is evident in these model findings.

4.5. Effects on climate

The implications of our study are that volcanic gas inputs to the atmosphere are primarily to the lower troposphere during effusive lava flows but that explosive pyroclastic eruptions such as the type that may have formed Scathach Fluctus could be more common than previously assumed. Even though the generation of buoyant volcanic plumes seems plausible from high elevation vents, such as the ~28 km above MPR plume described as possible from Ma'at Mons in the previous section, it would appear that plumes reaching the cloud base (~48 km above MPR) require very tightly constrained combinations of conditions, a finding which has also been noted in previous work (e.g. Glaze, 1999; Glaze et al., 2011; Thornhill, 1993). These types of events are unlikely but conceivable and would require a combination of conditions including high altitude, high volatile, longer conduit, and/or small conduit radius. Therefore, even if they occur they are rare, and longer-term atmospheric circulation processes must be responsible for the regular introduction of volcanic gases to the upper troposphere, the cloud layers, and above the clouds.

However, should these buoyant plume forming volcanic events occur, rare or otherwise, they could have a profound impact on Venusian climate. Gases such as H_2O, CO_2 and SO_2 play a vital role in cloud chemistry, which strongly influences the radiation budget and planetary albedo. The addition of ash particles could be important in acting as cloud droplet nuclei. We therefore cannot rule out volcanic input of gases as the cause of the decadal SO_2 fluctuations seen in the Pioneer Venus Orbiter (Esposito, 1985) and Venus Express (Marcq et al., 2012) observations, although other plausible explanations such as atmospheric circulatory phenomena also exist.

4.6. Mass and H_2O fluxes to the atmosphere

The model results outlined in this work allow us to make some preliminary estimates of the flux of volcanic gases to Venus' lower

atmosphere. If Scathach Fluctus was produced by an explosive volcanic event from a conduit of 25 m radius, requiring 4.5% H_2O as in the preceding case study (Section 4.3), the corresponding mean magma mass flux predicted by our model is $\sim 3 \times 10^8$ kg s^{-1}. Therefore, the estimated flux of H_2O to the atmosphere would be $\sim 14 \times 10^6$ kg s^{-1}. If the initial H_2O concentration is lower and compensated for with additional CO_2 (e.g. a 3% H_2O with 3% CO_2 mix), the corresponding mean magma mass and H_2O fluxes would be $\sim 3 \times 10^8$ kg s^{-1} and $\sim 9 \times 10^6$ kg s^{-1}, respectively. The estimated flux of H_2O from this, and other, explosive events at around MPR is therefore estimated to be of the order $\sim 10^7$ kg s^{-1}. This figure of course assumes a small conduit radius; larger conduits would produce correspondingly higher fluxes. Since eruptions of this style will have a high volatile output, one consequence of volcanic activity would be transient lateral variations of H_2O in Venus' near-surface atmosphere. Water vapour near the surface (at ~5–25 km altitude) can be measured from orbit, by analysing 1.18 μm thermal emission on the nightside of Venus. Such observations were carried out by the VIRTIS spectrometer on Venus Express, but analyses to date have not yet detected any spatial variability (Bézard et al., 2009), with a consistent H_2O concentration of 30 [−5 +10] ppm in Venus' altitude range 5–25 km above MPR (Bézard et al., 2011). This highlights the importance of the ongoing search for evidence of volcanic processes on Venus through remote sensing of atmospheric and surface properties.

4.7. Deposit emplacement, emissions, and limits of detectability

The mass flux estimates in Section 4.6, allow estimation of the duration of the emplacement of an explosive deposit of dimensions similar to Scathach Fluctus and the volcanic gas (H_2O) emission resulting from eruption. Our model shows that a mass flux of $> \sim 3 \times 10^8$ kg s^{-1} is required to sustain an explosive volcanic event at the altitude of Scathach Fluctus. Ghail and Wilson (2013) estimate the volume of Scathach Fluctus to be 225–875 km^3, and the density to be close to 2000 kg m^{-3}, consistent with a welded ignimbrite (Lepetit et al., 2009). Assuming a dense rock equivalent density of 2800 kg m^{-3}, this implies ~30% void space. Therefore, to generate a volume of pyroclastic ejecta equivalent to the lower end of this estimate, a minimum of ~150 km^3 or $\sim 4 \times 10^5$ Mt of magma must have been erupted. At a mass flux of $\sim 3 \times 10^8$ kg s^{-1}, the time to form Scathach Fluctus would be ~15 days. Given the inferred H_2O concentrations of 3–4.5%, $\sim 4 \times 10^5$ Mt of magma would release $\sim 1–2 \times 10^4$ Mt of H_2O over the duration of the eruption. The upper volume estimate however, implies an eruption sustained over a longer period of time in order to generate the additional material and/or a higher mass flux, generating more material per unit time. It is worth restating here the limitations of the steady-state, parallel-sided nature of the model and the consequences on the applicability of the model to long-term processes mentioned in Section 4.1. It is also worth noting that the deposit may have been emplaced by more than one event. However, this first-order analysis remains informative.

These findings coupled with the H_2O measurements, described by Bézard et al. (2009,2011), offer an opportunity for detecting volcanic signatures. Any perturbations to the consistent and low background concentration would be suggestive of an H_2O source to Venus' atmosphere. Spatial resolution of near-infrared nightside sounding of the surface is limited to ~90–100 km, due to multiple scattering in the cloud deck (Hashimoto and Imamura, 2001); for water vapour mapping at altitudes of 10–20 km, the spatial resolution might therefore be expected to be of order 60–70 km due to the closer proximity to the main cloud deck at 50 km altitude. The flux of H_2O will be dissipated by ambient winds, but the mean wind speed in the 0–20 km altitude range is only ~10 m s^{-1} (Kerzhanovich and Limaye, 1985), so the mean residence time of air in this reference volume of 70 km diameter (to approximate the spatial footprint of near-IR water vapour sounding) would be about 2 h. The pattern and rate of dissipation of the plume will depend on local atmospheric conditions, but if we assume that the emitted water vapour becomes well mixed over the lowest 20 km of the atmosphere and over a circular footprint of 70 km diameter, enough water vapour is emitted in 2 h to double the amount of water vapour found in this volume, from an initial assumed concentration of 30 ppm to 60 ppm. This suggests that local concentrations of 60 ppm could be sustained for as long as the eruption continues, even when averaged over the spatial blurring distance of the near-IR sounding footprint. A further inference that can be made from this finding is that, if a detection of this magnitude is made, the volatile concentrations required to cause this anomaly are more likely to have resulted in a buoyant column at very high elevations or a collapsing column at low elevations. Therefore, clues to the style of the eruption can be gathered from the elevation of the region above which the detection was made. While a thorough assessment of the detectability of such a plume would require more detailed consideration of plume dissipation mechanisms and rates, this first-order estimate of detectability suggests a renewed focus on analysis of the VIRTIS-M-IR dataset to search for near-surface water vapour variations.

5. Conclusions

By integrating the degassing model SolEx, geochemical lander data, measured atmospheric temperature and pressure profiles, and incorporating CO_2 as an accessory volatile to H_2O, we simulated a broad range of Venusian volcanic eruption scenarios. We found that the addition of CO_2 to an H_2O-driven eruption increases the final pressure, velocity, and volume fraction gas, the latter with an initial drop at a small initial addition of the accessory volatile. Increasing elevation is conducive to a greater degree of magma fragmentation, due to the decrease in final pressure at the vent, resulting in a greater likelihood of explosive activity. The effect of increasing the magmatic temperature is to generate higher final pressures, greater velocities, and lower final volume fraction gas values with a correspondingly lower chance of explosive volcanism. Conduit geometry was found to be important, with cross-sectionally smaller and/or deeper conduits more conducive to explosive activity.

Two case studies highlight the strong influence of elevation on the likelihood of explosive activity. If explosive in nature, Scathach Fluctus at Venus' MPR requires 4.5% H_2O (from a 25 m radius conduit) in order to initiate magmatic fragmentation, whereas the highest peak, Ma'at Mons, requires less than half that concentration (i.e. 2% H_2O). It is also found that conditions that barely generate explosive behaviour at the MPR (4.5% H_2O or 3% each of H_2O and CO_2) are very close to those capable of generating not only explosive behaviour, but a buoyant volcanic column (4.7% H_2O or 3% H_2O with 3% CO_2) reaching up to ~20 km at the summit of Ma'at Mons.

Volcanic input to Venus' atmosphere is considered a potentially important contributor to climatic processes on Venus. A relatively large global input to the lower atmosphere via small effusive eruptions, passive degassing, and pyroclastic events is likely to be the dominant volcano-atmosphere input. This modelling shows however, that the injection of volcanic material to higher atmospheric layers is feasible, if likely infrequent, and could play important roles in cloud chemistry and longer-term climate trends such as the measured decadal SO_2 fluctuations.

The inferred mass fluxes and H_2O concentrations suggested by these models provide some preliminary numerical estimates of the introduction of volcanic gases to the lower atmosphere of

Venus. If we accept that Scathach Fluctus was produced by an explosive volcanic event from a conduit of 25 m radius, requiring 4.5% H_2O the estimated flux of H_2O to the atmosphere would be $\sim 14 \times 10^6$ kg s^{-1}. If the initial H_2O concentration is lower, and compensated for with additional CO_2 (e.g. 3% H_2O with 3% CO_2), the H_2O flux would be $\sim 9 \times 10^6$ kg s^{-1}. Larger conduits and volcanic complexes would produce correspondingly higher fluxes. A sustained eruption of the scale of Scathach Fluctus could supply considerable quantities of H_2O to the atmosphere locally, over the course of the eruption. Despite the spatial blurring of the near-IR mapping of water vapour in the lower atmosphere, and the dissipation of emissions via wind, we conclude that a sustained eruption with a flux of $\sim 10^7$ kg s^{-1} of magma could double the mean H_2O abundance even over the $\sim$70 km spatial resolution of near-IR mapping of water vapour in the deep atmosphere, which is a large enough signal to be detectable. Continued search for spatial and temporal variations in H_2O in the Venus Express/VIRTIS dataset is therefore recommended, as the ability for measurements to detect volcanic signatures is supported by these model conclusions.

Acknowledgements

M. Airey would like to thank the staff and his colleagues at the Department of Earth Sciences, University of Oxford for academic support, two anonymous reviewers whose comments improved the final manuscript, and the Science and Technology Facilities Council for funding the postgraduate research project, of which this paper forms a part. (STFC grant number ST/I505880/1) C. Wilson acknowledges funding from the European Union Seventh Framework Program (FP7/2007-2013) under grant agreement no 606798 (EuroVenus).

References

Bézard, B., Fedorova, A., Bertaux, J.L., Rodin, A., Korablev, O., 2011. The 1.10- and 1.18-μm nightside windows of Venus observed by SPICAV-IR aboard Venus Express. Icarus 216, 173–183.
Bézard, B., Tsang, C.C.C., Carlson, R.W., Piccioni, G., Marcq, E., Drossart, P., 2009. Water vapor abundance near the surface of Venus from Venus Express/VIRTIS observations. J. Geophys. Res. Planets, 114.
Campbell, B.A., Rogers, P.G., 1994. Bell Regio, Venus—integration of remote-sensing data and terrestrial analogs for geologic analysis. J. Geophys. Res. Planets 99, 21153–21171.
Crumpler, L.S., Aubele, J.C., 2000. Volcanism on Venus. In: Sigurdsson, H. (Ed.), Encyclopedia of Volcanoes. Academic Press, San Diego, pp. 727–769.
De Bergh, C., Bezard, B., Owen, T., Crisp, D., Maillard, J.P., Lutz, B.L., 1991. Deuterium on Venus—observations from Earth. Science 251, 547–549.
Diez, M., 2006. Solution and parametric sensitivity study of a coupled conduit and eruption column model. In: Mader, H.M., Coles, S.G., Connor, C.B., Connor, L.J. (Eds.), Statistics in Volcanology. The Geological Society, London.
Dixon, J.E., 1997. Degassing of alkalic basalts. Am. Mineral. 82, 368–378.
Donahue, T.M., 1999. New analysis of hydrogen and deuterium escape from Venus. Icarus 141, 226–235.
Donahue, T.M., Hoffman, J.H., Hodges, R.R., Watson, A.J., 1982. Venus was wet: a measurement of the ratio of deuterium to hydrogen. Science 216.
Elkins-Tanton, L.T., Smrekar, S.E., Hess, P.C., Parmentier, E.M., 2007. Volcanism and volatile recycling on a one-plate planet: applications to Venus. J. Geophys. Res. Planets 112.
Esposito, L.W., 1985. Long term changes in Venus sulfur dioxide. Adv. Space Res. 5, 85–90.
Fagents, S.A., Wilson, L., 1995. Explosive volcanism on Venus: transient volcanic explosions as a mechanism for localized pyroclast dispersal. J. Geophys. Res. Planets 100, 26327–26338.
Ford, J.P., Plaut, J.J., Weitz, C.M., Farr, T.G., Senske, D.A., Stofan, E.R., Michaels, G., Parker, T.J., 1993. Guide to Magellan Image Interpretation. JPL, Pasadena, CA.
Ghail, R.C., Wilson, L., 2013. A pyroclastic flow deposit on Venus. Geological Society, vol. 401. Special Publications, London.
Ghiorso, M.S., Sack, R.O., 1995. Chemical mass-transfer in magmatic processes. IV: A revised and internally consistent thermodynamic model for the interpolation and extrapolation of liquid–solid equilibria in magmatic systems at elevated temperatures and pressures. Contrib. Mineral. Petrol. 119, 197–212.
Giordano, D., Russell, J.K., Dingwell, D.B., 2008. Viscosity of magmatic liquids: a model. Earth Planet. Sci. Lett. 271, 123–134.
Glaze, L.S., 1999. Transport of SO_2 by explosive volcanism on Venus. J. Geophys. Res. Planets 104, 18899–18906.
Glaze, L.S., Baloga, S.M., Wilson, L., 1997. Transport of atmospheric water vapor by volcanic eruption columns. J. Geophys. Res. Atmos. 102, 6099–6108.
Glaze, L.S., Baloga, S.M., Wimert, J., 2011. Explosive volcanic eruptions from linear vents on Earth, Venus, and Mars: comparisons with circular vent eruptions. J. Geophys. Res. Planets, 116.
Gonnermann, H.M., Manga, M., 2003. Explosive volcanism may not be an inevitable consequence of magma fragmentation. Nature 426, 432–435.
Gonnermann, H.M., Manga, M., 2012. Dynamics of magma ascent in the volcanic conduit. In: Fagents, S.A., Gregg, T.K.P., Lopes, R.M.C. (Eds.), Modeling Volcanic Processes: The Physics and Mathematics of Volcanism. Cambridge University Press, Cambridge.
Grinspoon, D.H., 1993. Implications of the high D/H ratio for the sources of water in Venus atmosphere. Nature 363, 428–431.
Grosfils, E.B., Long, S.M., Venechuk, E.M., Hurwitz, D.M., Richards, J.W., Kastl, B., Drury, D.E., Hardin, J., 2011. Geologic Map of the Ganiki Planitia Quadrangle (V-14), Venus [map], Scientific Investigations Map 3121. U.S. Geological Survey.
Haar, L., Gallagher, J.S., Kell, G.S., 1984. NBS/NRC Steam Tables. Hemisphere Publishing Corporation, New York, NY.
Hashimoto, G.L., Imamura, T., 2001. Elucidating the rate of volcanism on Venus: detection of lava eruptions using near-infrared observations. Icarus 154, 239–243.
Head, J.W., Crumpler, L.S., Aubele, J.C., Guest, J.E., Saunders, R.S., 1992. Venus volcanism—classification of volcanic features and structures, associations, and global distribution from magellan data. J. Geophys. Res. Planets 97, 13153–13197.
Ivanov, M.A., Head, J.W., 2011. Global geological map of Venus. Planet. Space Sci. 59, 1559–1600.
Kaula, W.M., 1999. Constraints on Venus evolution from radiogenic argon. Icarus 139, 32–39.
Keddie, S.T., Head, J.W., 1995. Formation and evolution of volcanic edifices on the Dione-Regio rise, Venus. J. Geophys. Res. Planets 100, 11729–11754.
Kerzhanovich, V.V., Limaye, S.S., 1985. Circulation of the atmosphere from the surface to 100 km. Adv. Space Res. 5, 59–83.
Lepetit, P., Viereck-Goette, L., Schumacher, R., Mues-Schumacher, U., Abratis, M., 2009. Parameters controlling the density of welded ignimbrites—a case study on the Incesu Ignimbrite, Cappadocia, Central Anatolia. Chem. Erde 69, 341–357.
Lesne, P., Kohn, S.C., Blundy, J., Witham, F., Botcharnikov, R.E., Behrens, H., 2011. Experimental simulation of closed-system degassing in the system basalt-H_2O–CO_2–S–Cl. J. Petrol. 52, 1737–1762.
Marcq, E., Bertaux, J.L., Montmessin, F., Belyaev, D., 2012. Variations of sulphur dioxide at the cloud top of Venus's dynamic atmosphere. Nat. Geosci., 1–4.
Mastin, L.G., Ghiorso, M.S., 2000. A Numerical Program for Steady-state Flow of Magma-gas Mixtures through Vertical Eruptive Conduits. Open-file Report 00-209. U.S. Department of the Interior. USGS, Vancouver, WA.
McGill, G.E., 2000. Geolgic Map of the Sappho Patera Quadrangle (V-20), Venus [map], Geologic Investigations Series I-2637. U.S. Geological Survey.
McGovern, P.J., Solomon, S.C., 1998. Growth of large volcanoes on Venus: mechanical models and implications for structural evolution. J. Geophys. Res. Planets 103, 11071–11101.
Mitchell, K.L., 2005. Coupled conduit flow and shape in explosive volcanic eruptions. J. Volcanol. Geotherm. Res. 143, 187–203.
Morton, B.R., Taylor, G., Turner, J.S., 1956. Turbulent gravitational convection from maintained and instantaneous sources. Proc. R. Soc. London, Ser. A Math. Phys. Sci. 234, 1–23.
Mueller, N., Helbert, J., Hashimoto, G.L., Tsang, C.C.C., Erard, S., Piccioni, G., Drossart, P., 2008. Venus surface thermal emission at 1 μm in VIRTIS imaging observations: evidence for variation of crust and mantle differentiation conditions. J. Geophys. Res. Planets 113.
Newman, S., Lowenstern, J.B., 2002. VOLATILECALC: a silicate melt-H_2O–CO_2 solution model written in Visual Basic for excel. Comput. Geosci. 28, 597–604.
Nimmo, F., McKenzie, D., 1998. Volcanism and tectonics on Venus. Annu. Rev. Earth Planet. Sci. 26, 23–51.
Papale, P., 1999. Strain-induced magma fragmentation in explosive eruptions. Nature 397, 425–428.
Papale, P., Dobran, F., 1994. Magma flow along the volcanic conduit during the plinian and pyroclastic flow phases of the may 18, 1980, Mount-St-Helens eruption. J. Geophys. Res. Solid Earth 99, 4355–4373.
Papale, P., Moretti, R., Barbato, D., 2006. The compositional dependence of the saturation surface of H_2O+CO_2 fluids in silicate melts. Chem. Geol. 229, 78–95.
Papale, P., Neri, A., Macedonio, G., 1998. The role of magma composition and water content in explosive eruptions—1. Conduit ascent dynamics. J. Volcanol. Geotherm. Res. 87, 75–93.
Papale, P., Polacci, M., 1999. Role of carbon dioxide in the dynamics of magma ascent in explosive eruptions. Bull. Volcanol. 60, 583–594.
Pavri, B., Head, J.W., Klose, K.B., Wilson, L., 1992. Steep-sided domes on Venus—characteristics, geologic setting, and eruption conditions from magellan data. J. Geophys. Res. Planets 97, 13445–13478.
Robinson, C.A., Thornhill, G.D., Parfitt, E.A., 1995. Large-scale volcanic activity at Maat-Mons—can this explain fluctuations in atmospheric chemistry observed by Pioneer-Venus? J. Geophys. Res. Planets 100, 11755–11763.
Scandone, R., Malone, S.D., 1985. Magma supply, magma discharge and readjustment of the feeding system of Mount St Helens during 1980. J. Volcanol. Geotherm. Res. 23, 239–262.

Seiff, A., Schofield, J.T., Kliore, A.J., Taylor, F.W., Limaye, S.S., Revercomb, H.E., Sromovsky, L.A., Kerzhanovich, V.V., Moroz, V.I., Marov, M.Y., 1985. Models of the structure of the atmosphere of Venus from the surface to 100 kilometers altitude. Adv. Space Res. 5, 3–58.
Shellnutt, J.G., 2013. Petrological modeling of basaltic rocks from Venus: a case for the presence of silicic rocks. J. Geophys. Res. Planets 118, 1350–1364.
Sparks, R.S.J., 1978. The dynamics of bubble formation and growth in magmas—a review and analysis. J. Volcanol. Geotherm. Res. 3, 1–37.
Sparks, R.S.J., 1986. The dimensions and dynamics of volcanic eruption columns. Bull. Volcanol. 48, 3–15.
Stofan, E.R., Anderson, S.W., Crown, D.A., Plaut, J.J., 2000. Emplacement and composition of steep-sided domes on Venus. J. Geophys. Res. Planets 105, 26757–26771.
Taylor, F.W., 2010. Planetary Atmospheres. Oxford University Press, Oxford.
Thornhill, G.D., 1993. Theoretical modeling of eruption plumes on Venus. J. Geophys. Res. Planets 98, 9107–9111.
Treiman, A.H., 2007. Geochemistry of Venus' surface: current limitations as future opportunities. In: Esposito, L.W., Stofan, E.R., Cravens, E. (Eds.), Exploring Venus as a Terrestrial Planet: Geophysical Monograph, vol. 176. American Geophysical Union, Washington, DC.
Tuffen, H., Dingwell, D., 2005. Fault textures in volcanic conduits: evidence for seismic trigger mechanisms during silicic eruptions. Bull. Volcanol. 67, 370–387.
Valentine, G.A., Wohletz, K.H., 1989. Numerical-models of plinian eruption columns and pyroclastic flows. J. Geophys. Res. Solid Earth Planets 94, 1867–1887.
Wallace, P.J., 2005. Volatiles in subduction zone magmas: concentrations and fluxes based on melt inclusion and volcanic gas data. J. Volcanol. Geotherm. Res. 140, 217–240.
Wilson, L., Sparks, R.S.J., Huang, T.C., Watkins, N.D., 1978. The control of volcanic column heights by eruption energetics and dynamics. J. Geophys. Res. 83, 1829–1836.
Wilson, L., Sparks, R.S.J., Walker, G.P.L., 1980. Explosive volcanic eruptions. 4. The control of magma properties and conduit geometry on eruption column behavior. Geophys. J. R. Astron. Soc. 63, 117–148.
Witham, F., Blundy, J., Kohn, S.C., Lesne, P., Dixon, J., Churakov, S.V., Botcharnikov, R., 2012. SolEx: a model for mixed COHSCl-volatile solubilities and exsolved gas compositions in basalt. Comput. Geosci. 45, 87–97.
Woods, A.W., 1988. The fluid dynamics and thermodynamics of eruption columns. Bull. Volcanol. 50, 169–193.
Woods, A.W., 1995. The dynamics of explosive volcanic eruptions. Rev. Geophys. 33, 495–530.
Woods, A.W., Bower, S.M., 1995. The decompression of volcanic jets in a crater during explosive volcanic-eruptions. Earth Planet. Sci. Lett. 131, 189–205.
Zhang, Y.X., 1999. A criterion for the fragmentation of bubbly magma based on brittle failure theory. Nature 402, 648–650.